



HAL
open science

Pyrazolones as inhibitors of immune checkpoint blocking the PD-1/PD-L1 interaction

Raphaël Le Biannic, Romain Magnez, Frédérique Klupsch, Natascha Leleu-Chavain, Bryan Thiroux, Morgane Tardy, Hassiba El Bouazzati, Xavier Dezitter, Nicolas Renault, Gérard Vergoten, et al.

► To cite this version:

Raphaël Le Biannic, Romain Magnez, Frédérique Klupsch, Natascha Leleu-Chavain, Bryan Thiroux, et al.. Pyrazolones as inhibitors of immune checkpoint blocking the PD-1/PD-L1 interaction. *European Journal of Medicinal Chemistry*, 2022, 236, pp.114343. 10.1016/j.ejmech.2022.114343 . hal-03641793

HAL Id: hal-03641793

<https://hal.science/hal-03641793v1>

Submitted on 22 Jul 2024

HAL is a multi-disciplinary open access archive for the deposit and dissemination of scientific research documents, whether they are published or not. The documents may come from teaching and research institutions in France or abroad, or from public or private research centers.

L'archive ouverte pluridisciplinaire **HAL**, est destinée au dépôt et à la diffusion de documents scientifiques de niveau recherche, publiés ou non, émanant des établissements d'enseignement et de recherche français ou étrangers, des laboratoires publics ou privés.



Distributed under a Creative Commons Attribution - NonCommercial 4.0 International License

Pyrazolones as Inhibitors of Immune Checkpoint Blocking the PD-1/PD-L1 Interaction

Raphaël Le Biannic,^a Romain Magnez,^b Frédérique Klupsch,^a Natascha Leleu-Chavain,^a
Bryan Thiroux,^b Morgane Tardy,^b Hassiba El Bouazzati,^b Xavier Dezitter,^a Nicolas Renault,^a
Gérard Vergoten,^a Christian Bailly,^c Bruno Quesnel,^b Xavier Thuru,^{b+*} Régis Millet,^{a+*}

^a Univ. Lille, Inserm, U1286 - INFINITE - Lille Inflammation Research International Center, ICPAL, 3 rue du Professeur Laguesse, 59000 Lille, France

^b Univ. Lille, CNRS, Inserm, CHU Lille, UMR9020 – UMR1277 - Canther – Cancer Heterogeneity, Plasticity and Resistance to Therapies, 1 place de Verdun, 59000 Lille, France

^c Oncowitan, Lille, France

RECEIVED DATE (to be automatically inserted after your manuscript is accepted if required according to the journal that you are submitting your paper to)††

† These authors contributed equally *Correspondence: Pr. Régis Millet, Phone, +33 3 20 96 43 74; fax, +33 3 20 96 49 06; e-mail: regis.millet@univ-lille.fr and Dr. Xavier Thuru, Phone, +33 3 20 16 92 15; e-mail : xavier.thuru@univ-lille.fr.

ABSTRACT

Immuno-therapy has become a leading strategy to fight cancer. Over the past few years, immuno-therapies using checkpoint inhibitor monoclonal antibodies (mAbs) against programmed death receptor 1 (PD-1) and programmed death ligand 1 (PD-L1) have demonstrated improved survival compared with chemotherapy. We describe the microwave-assisted synthesis and the characterization of an innovative series of synthetic compounds endowed with nanomolar activity against PD-L1. The properties of the compounds were characterized using several biophysical techniques including microscale thermophoresis (MST) and fluorescence resonance energy transfer (FRET) measurements. A few small molecules demonstrated a high affinity for human PD-L1, potently disrupted the PD-L1:PD-1 interaction and inhibited Src homology region 2 domain-containing phosphatase (SHP2) recruitment to PD-1. More than 30 molecules from the pyrazolone family have been synthesized and 5 highly potent “PD-L1 silencing compounds” have been identified, based on

in vitro measurements. Structure-activity relationships have been defined and ADME properties were evaluated. The phenyl-pyrazolone unit offers novel perspectives to design PD-L1-targeting agents, potentially useful to combat cancer and other pathologies implicating the PD-1/PD-L1 checkpoint.

KEYWORDS: Pyrazolones, PD-1/PD-L1, Immune checkpoints, Proteins, Cancer

INTRODUCTION

Before the age of 70, cancer is the first or second leading cause of death in 112 countries throughout the world. Overall, the cancer incidence is increasing worldwide. A 47% increase is expected between 2020 and 2040 [1] due to demographic changes accentuated by urbanization and its associated effects such as pollution, diet pattern and longer life span. Major progresses in the treatments have been made over the past three decades. Chemoradiotherapy is currently the most used treatment approach [2] but it has its limitation with severe side effects and the development of resistant cancer cells which can cause relapsing, often deadly [3]. Cancer immunotherapy is a more recent successful approach to eliminate cancer cells by enhancing or modulating the host immune system [4]. The main targets of this strategy are the immune checkpoints. Normally, they regulate the amplitude of the immune response and reduce collateral tissue damage. In some cases, cancer cells interact with immune checkpoints which inhibit the immune response and thus favor the development of tumors.

PD-1 is one of the main targets of cancer immunotherapy [5]. PD-1 is a transmembrane receptor expressed on the surface of T cells, B cells, monocytes, natural killer T cells and dendritic cells. It has two natural ligands: PD-L1 and PD-L2. PD-L1 is overexpressed on the cell surface of different tumors [6] and allows them to escape T cells lysis [7]. The PD-L1/PD-1 association induces many inhibitory processes of the immune response. It inhibits the proliferation of T cells, inhibit cytokines production and induce T cell apoptosis [2]. It also impairs T-cell antigen recognition [8]. Targeting this interaction could allow the restoration of T cells activity and recognition of malignant cells by the immune system. Currently, the only compounds blocking the interaction between PD-1 and PD-L1 approved or at an advanced stage of development are monoclonal antibodies (mAb, such as nivolumab, atezolizumab, and several others). They have drastically improved the survival rates of advanced, aggressive cancers (in particular melanoma and non-small cell lung cancer) [9]. Targeting PD-L1 instead of PD-1 has proven to be a more specific and efficient strategy

associated to less severe side effects [10,11]. Despite their high affinity, monoclonal antibodies have several drawbacks such as poor bioavailability, poor tumor penetration, expensive production and specific mAb-related toxicities [12]. Moreover, the blood-brain barrier strongly limits the entry of monoclonal antibodies in the normal brain [13]. Small molecules blocking the interaction between PD-1 and PD-L1 could be orally available, cheaper to produce than mAb while presenting improved pharmacokinetics with greater diffusion rate [14]. However, because of the large and relatively flat hydrophobic interaction surface of the PD-1/PD-L1 complex [15], thus far the development of small molecules has lagged far behind the development of therapeutic biomolecules.

Today, relatively few small molecules targeting the PD-L1/PD-1 interaction have been described. Bristol-Myers Squibb (Figure 1) was the first to design and develop PD-L1-targeted small molecules containing a biphenyl core scaffold [16].

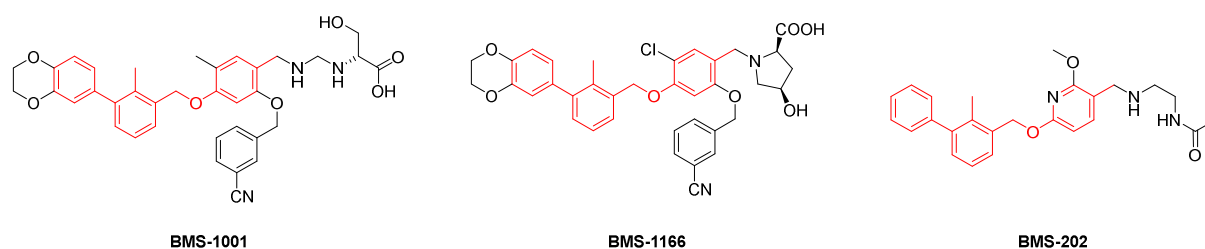


Figure 1. Example of PD-L1-targeted compounds developed by BMS based on a biphenyl scaffold

A few other companies and academic groups have reported small molecules directed against PD-L1. For example, Arbutus Biopharma Inc. described anti-PD-L1 small molecules which were shown to induce a 60.4% tumor volume reduction in a colorectal cancer model *in vivo*. These small molecules could also enhance immune response against the hepatitis B virus [17]. Aurigene Discovery in collaboration with Curis has designed and optimized a 29-mer peptide based on the structure of *h*PD-1 targeting PD-L1, **AUNP-12** (Figure 2), precursor of **CA-170**, a peptidomimic. Although its capacity to target only PD-L1 has been questioned [14], **CA-170** is in clinical studies, undergoing phase I clinical trials for the treatment of advanced solid tumors and lymphomas and phase II clinical trials for the treatment of lung cancer, head and neck/oral cavity cancer, MSI-H positive cancers and Hodgkin lymphoma in India.[14]. In recent years, different series of small molecules targeting PD-L1 and/or the PD-L1/PD-1 interface have been described [18-21] and some other compounds are currently in clinical

studies like **INCB086550**, developed by Incyte (US), actually in phase II clinical trials (NCT04629339/NCT03762447) or **IMMH-010**, developed by Tianjin Chasesun (China), in phase I clinical trials for the treatment of selected solid tumors (NCT04343859) [22-23]. Wang M. et al. have also discovered pyrrole-imidazole polyamides as PD-L1 expression inhibitors targeting PD-1/PD-L1 interaction [24]. Song Z. et al. have designed biaryl [25] bearing a unique difluoromethyleneoxy linkage (compound A, figure 2) and Wang T. et al have described a biphenyl pyridine (compound B) [26] and a biphenyl oxadiazol compound (compound C, figure 2) that promote PD-L1 internalization and degradation [27].

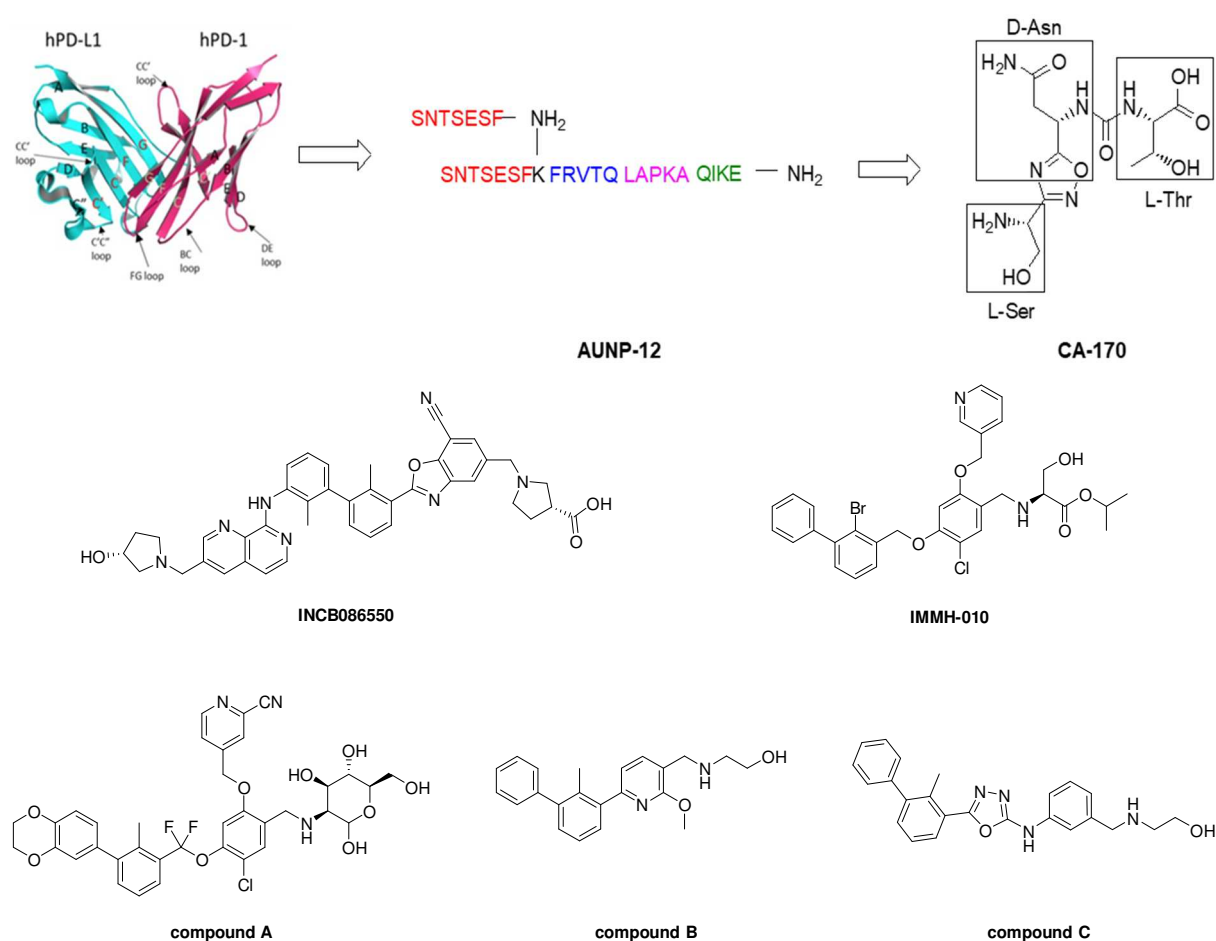


Figure 2. Description of the advancement of PD-L1 inhibitors. Structures of **AUNP-12**, a peptide based on the structure of 4 *hPD-1* parts (2 BC loops in red, the D strand in blue, the FG loop in pink and the G strand in green), **CA-170**, **INCB086550**, **IMMH-010**, **compound A**, **compound B** and **compound C**.

In an attempt to identify new derivatives, a screening of a small in-house chemical library was undertaken to identify PD-L1 ligands. Two relevant and complementary methodologies were

used for the screening: (i) a MicroScale Thermophoresis (MST) *in vitro* assay and (ii) a cell-based Förster Resonance Energy Transfer (FRET) assay. MST is a powerful method for the quantitative analysis of protein-ligand interactions with low sample consumption based on the motion of molecules along local temperature gradients, useful to evaluate compounds affinity for PD-L1 (K_D) as described previously [28]. FRET assay allowed to evaluate the capacity of compounds to potently disrupt the PD-L1:PD-1 interaction and to inhibit Src homology region 2 domain-containing phosphatase (SHP2, the down-stream effector protein) recruitment to PD-1.

Two hundred molecules were screened which resulted in the identification of multiple hits with K_D in the submicromolar range. We selected an interesting hit compound including a phenyl-pyrazolone core structure (compound **2**) and then we designed, synthesized and tested a complete series of bi-substituted pyrazolone derivatives (**3-40**) with the objective to enhance activity and affinity for PD-L1 and to establish structure-activity relationships in the series (Figure 3).

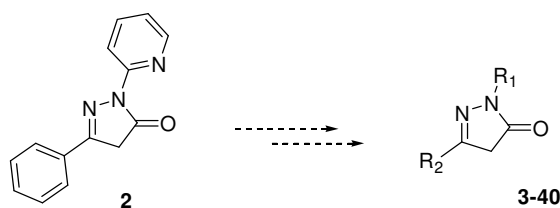


Figure 3. General structure of synthesized pyrazolones (**2-40**)

RESULTS AND DISCUSSION

Chemistry.

Pyrazolones were synthesized by the Knorr reaction, a condensation between an hydrazine and a β -keto ester [29]. Multiple protocols have been described using microwaves [30, 31], sonication [30, 32] in different solvents such as a mix of ethanol and glacial acetic acid [30], glacial acetic acid only [33] or without any solvents [31, 32]. Here, the reaction was carried out by sonication in a concentrated acetic acid medium since it induced a precipitation of the desired product. Therefore, we could observe an improved yield, short reaction times with easy work-up compared to other protocols. With alkyl β -keto esters, the sonication protocol resulted in poor yields, therefore microwaves (150W, 130°C) were used (Figure 4).

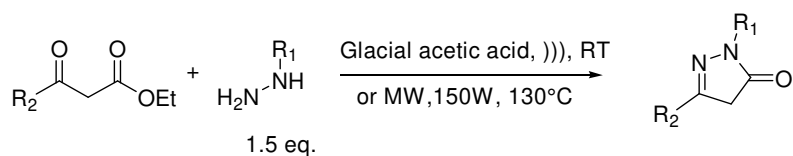


Figure 4. Synthesis of the pyrazolones by sonication for aromatic and adamantane compounds (R_2 = aromatic or adamantane groups) and microwaves activation for alkyl compounds (R_2 = alkyl groups)

The desired β -keto esters were synthesized by various methods depending on the starting materials availability (Figure 5). Three methods were investigated. Method A consists in a Claisen condensation between a ketone precursor with diethyl carbonate in presence of sodium hydride in anhydrous toluene (compounds **1a-c**) (Figure 6) [34].

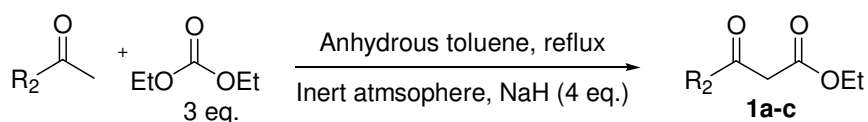


Figure 5. Synthesis of β -keto esters using the method A

For the method B, ethyl potassium malonate is *C*-acylated by an acyl chloride precursor in presence of a magnesium chloride-triethylamine base system (**1d-e**) (Figure 6) [35].

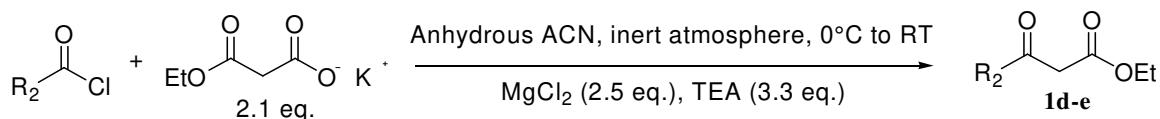


Figure 6. Synthesis of β -keto esters using the method B

Method C is a two steps reaction. First, the ester is activated with dicyclohexylcarbodiimide and 4-dimethylaminopyridine as a catalyst in anhydrous dichloromethane. The active ester acylates Meldrum's acid to give the corresponding acyl Meldrum's acid intermediate. Then, in the presence of ethanol and *p*-toluenesulfonic acid as a catalyst, this intermediate decomposes into carbon dioxide, acetone and the desired β -keto ester (**1f**) (Figure 7) [36].

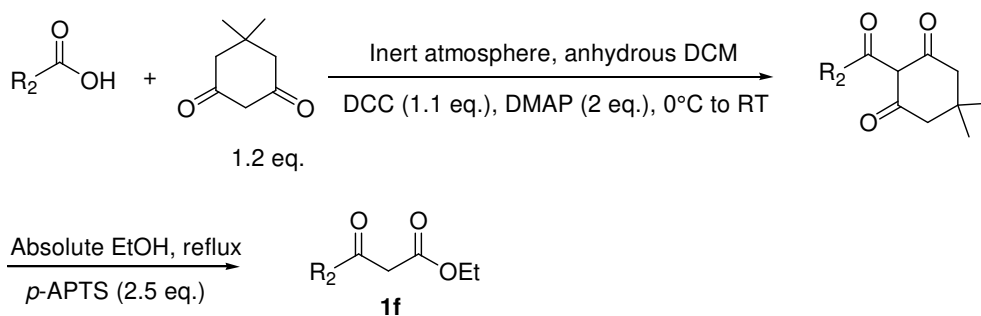


Figure 7. Synthesis of β -keto esters using the method C

The three methods (A, B and C) led to the synthesis of the full range of compounds (**3-40**), all obtained in a satisfactory yield and fully characterized by $^1\text{H-NMR}$, $^{13}\text{C-NMR}$, LC-MS and HRMS. We designed bi-substituted pyrazolone derivatives bearing i) in R_1 an unsubstituted pyridine (connected *via* position 2, 3, or 4), a mono- or di-substituted pyridine connected *via* the 2-position, a mono- or di-substituted phenyl (halogen, methyl, amino or methoxy) or a pyrimidine connected *via* the 2-position and ii) in R_2 a mono or polysubstituted phenyl ring (methoxy, halogen, trifluoromethyl, nitro, methyl), a linear aliphatic chain (methyl, ethyl, propyl and butyl), a branched aliphatic chain (isopropyl and *tert*-butyl) or a non-aromatic group (adamantyl). All compounds were evaluated as potential PD-L1 binders, using the aforementioned MST and FRET assays.

Structure-activity relationships.

We started from the hit compound **2** identified during the initial screening procedure. This phenyl-pyrazole-pyridine unfused tricyclic compound is a potent PD-L1 binder, characterized by a K_D (MST) of 385 nM and an IC_{50} (FRET) of 359 nM. From this compound, we modulated the phenyl and pyridine rings (R_1 , R_2) on both side of the pyrazolone core to establish structure-activity relationships (SAR).

To begin with, the 2-pyridine unit was maintained (R_1) as in compound **2** while modifications on the other side (R_2) were carried out. A phenyl substituent was selected for the R_2 group and the three positions, *ortho*, *meta*, and *para*, were investigated. For the *ortho* position, the substitution by a methoxy group (compound **3**) significantly increases affinity (17-folds higher, K_D (MST) = 23 nM) and activity (50-folds higher, IC_{50} (FRET) = 7.0 nM) of the resulting molecule **3** compared to compound **2**. Other *ortho* substitutions by a Cl or F atom, or a Me group (compounds **4-6**) resulted in a major loss of affinity. For the *meta* position, the substitution by a methoxy group, a Cl atom, a Me or CF_3 group, with diverse steric and

electronic effects resulted in a total loss of affinity (compounds **7-9**) or in a drastic reduction of potency (compound **10**). Similarly, to the *ortho* position, compound **11** substituted with a methoxy group at the *para* position, is more potent than compound **2** (K_D 4-folds higher and IC_{50} 21-folds higher) but less potent than compound **3**. Substitution by a CF_3 group at the *para* position (compound **12**) also induced an increase of affinity and activity compared to compound **2** but not as much as the methoxy substitution (compound **11**). The other compounds with a Cl atom, a Me or NO_2 group, or a F atom at the *para* position showed a poor (compounds **13-14**) or no (compounds **15-16**) affinity for PD-L1. In summary, modifications on the phenyl ring of the R_2 group allowed to determine the favorable substituents for PD-L1 affinity and activity: a methoxy group at the *ortho* or *para* positions of the phenyl give the most potent inhibitors (compounds **3** and **11**).

Multi-substituted phenyl compounds were also synthesized. Thereby, compound **17**, disubstituted with methoxy groups at the 3- and 4-positions showed a much better potency (K_D (MST) = 1.19 nM and IC_{50} (FRET) = 7.3 nM) than compound **2** (Figures 8 and 9) and the monosubstituted compounds **3** and **11**. This compound was shown also to bind to mouse PD-L1 ($1,63 \pm 0,5$ nM).

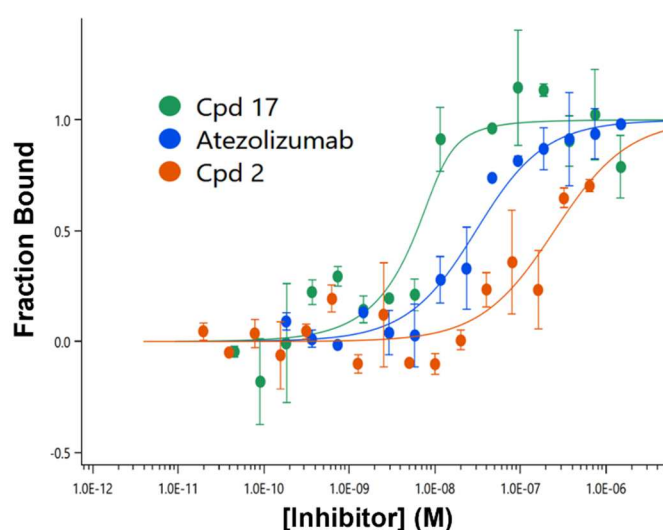


Figure 8. MST binding assay. Dose response curve between pyrazolones and rhPD-L1 (recombinant human PD-L1). Atezolizumab is used as reference compound, with a K_D value of 91 ± 7 nM (blue). PD-L1 is labelled with the Monolith His-tag labelling kit (NanoTemper). MST experiments were carried out at 100 % LED and low MST power. Graphs are represented as fraction bound against ligand concentration. The calculated K_D values were 1.19 ± 0.4 nM for compound **17** (green) and 385 ± 21 nM for compound **2** (orange). Data represent three independent experiments and were fitted to a K_D -binding model assuming a 1:1 binding stoichiometry.

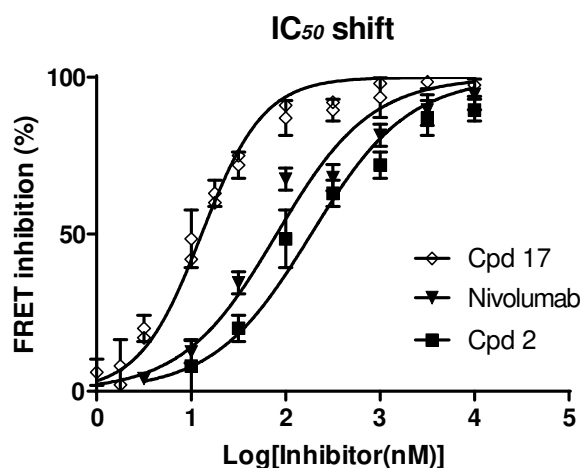


Figure 9. FRET inhibition using reporter cell-based assay. Nivolumab is used as reference (triangle). Various concentrations of pyrazolones were used to monitor FRET inhibition. After the addition of PD-L1 (10 μ M) to the co-transfected PD1-SHP2 cells, dose-response analyses are performed to determine the IC_{50} of the molecule under study. IC_{50} values were obtained using Graphpad software. IC_{50} value of **BMS-202** = 124 ± 12 nM. Data represent five independent experiments (n=5).

A trimethoxy molecule (compound **18**) was also synthesized but resulted in a total loss of affinity for PD-L1. Interestingly, despite the absence or poor affinity of chlorinated compounds **4**, **8** and **13**, the disubstitution by two Cl atoms at the *ortho* and *para* positions (compound **19**) was favorable for the affinity (K_D (MST) = 110 nM) and activity (IC_{50} (FRET) = 98 nM). However, compound **20** with two Cl atoms at the *meta* and *para* positions showed the same potency than the hit compound **2**. Finally, compound **21** with a mixed substitution (Cl atom at the *meta* position and methoxy at the *para* position) showed no affinity for PD-L1.

Then, alkyl chains were introduced for the R_2 group. Substitution by a methyl group (compound **22**) resulted in a good potency for PD-L1 (K_D (MST) = 77 nM and IC_{50} (FRET) = 92 nM). However, extending the chain to an ethyl (compound **23**), propyl (compound **24**) or butyl (compound **25**) group resulted in a massive loss of affinity. Similarly, compounds **26-27** with isopropyl and *tert*-butyl for R_2 showed no affinity. However, the introduction of an adamantane (compound **28**) resulted in a good affinity for PD-L1 (K_D (MST) = 340 nM) and a high activity (IC_{50} (FRET) = 4 nM). Finally, we observed no affinity with the symmetric compound **29** bearing two 2-pyridine groups. Thus, the modification of the R_2 substituent allowed the identification of six interesting compounds (**3**, **11**, **17**, **19**, **22** and **28**), with activity largely better than the hit compound **2** (IC_{50} (FRET) < 100 nM).

To complete this study, we moved on to modify the R₁ substituent while fixing the R₂ substituent as the adamantane group due to compound **28** revealing an IC₅₀ value in the nanomolar range. First, the position of the nitrogen of the 2-pyridine was changed and 3-pyridine (compound **30**) and 4-pyridine (compound **31**) derivatives were prepared. Unfortunately, these molecules showed no affinity for PD-L1. Other R₁ substituents were investigated as 2,4-diCl-phenyl (compound **32**), 2,4-diCH₃-phenyl (compound **33**), 2,4-diNH₂-phenyl (compound **34**), phenyl (compound **35**). Compound **32** with a 2,4-diCl-phenyl substituent revealed an excellent potency for PD-L1 (K_D (MST) = 19 nM and IC₅₀ (FRET) = 3 nM). We selected this latter potent compound for the ITC experiments (see below). Finally, the R₂ substituent was fixed as a 2-MeO-phenyl group and a series of substituted 2-pyridines were prepared. Results showed no affinity for the pyrimidine **36** and for the fluorinated (compounds **37-38**) and chlorinated 2-pyridines compounds (compounds **39-40**). It has been concluded that the 2-pyridine group is a pharmacophoric element for our PD-L1 inhibitors.

Table 1: Synthesized pyrazolones, their affinity (MST) and their bioactivity (FRET) for PD-L1.

Compounds	R ₁	R ₂	K _D (nM) MST	K _D (nM)	
				MST	IC ₅₀ (nM) FRET
2	2-pyridine	Phenyl	385 ± 21	-	359 ± 17
3	2-pyridine	2-MeO-phenyl	23 ± 5	46 ± 11	7 ± 4
4	2-pyridine	2-Cl-phenyl	>500 000	-	-
5	2-pyridine	2-Me-phenyl	>500 000	-	-
6	2-pyridine	2-F-phenyl	>500 000	-	-
7	2-pyridine	3-MeO-phenyl	NB	-	-
8	2-pyridine	3-Cl-phenyl	>500 000	-	-
9	2-pyridine	3-Me-phenyl	>500 000	-	-

10	2-pyridine	3-CF ₃ -phenyl	1200 ± 200	-	1100 ± 200
11	2-pyridine	4-MeO-phenyl	83 ± 12	2 ± 0,9	17 ± 5
12	2-pyridine	4-CF ₃ -phenyl	156 ± 12	-	143 ± 12
13	2-pyridine	4-Cl-phenyl	27000 ± 5000	-	33000 ± 7000
14	2-pyridine	4-Me-phenyl	1090 ± 0,2	-	-
15	2-pyridine	4-NO ₂ -phenyl	NB	-	-
16	2-pyridine	4-F-phenyl	NB	-	-
17	2-pyridine	3,4-diMeO-phenyl	1.19 ± 0.4	0,7 ± 0.2	7.3 ± 1.2
18	2-pyridine	3,4,5-triMeO-phenyl	NB	-	-
19	2-pyridine	2,4-diCl-phenyl	110 ± 17	-	98 ± 12
20	2-pyridine	3,4-diCl-phenyl	584 ± 75	-	-
21	2-pyridine	2-Cl-4-MeO-phenyl	NB	-	-
22	2-pyridine	Methyl	77 ± 7	53 ± 17	92 ± 9
23	2-pyridine	Ethyl	>500 000	-	-
24	2-pyridine	Propyl	>500 000	-	-
25	2-pyridine	Butyl	>500 000	-	-
26	2-pyridine	Isopropyl	>500 000	-	-
27	2-pyridine	<i>Tert</i> -butyl	>500 000	-	-
28	2-pyridine	Adamantane	340 ± 27	-	4 ± 2
29	2-pyridine	2-pyridine	>500 000	-	-
30	3-pyridine	Adamantane	NB	-	-
31	4-pyridine	Adamantane	NB	-	-
32	2,4-diCl-phenyl	Adamantane	19 ± 3	24 ± 11	9 ± 2
33	2,4-diCH ₃ -phenyl	Adamantane	NB	-	-
34	2,4-diNH ₂ -phenyl	Adamantane	NB	-	-
35	Phenyl	Adamantane	NB	-	-
36	2-pyrimidine	2-MeO-phenyl	NB	-	-
37	3-F-2-pyridine	2-MeO-phenyl	NB	-	-

	38	3,5-diF-2- pyridine	2-MeO-phenyl	NB	-	-	
	39	4-Cl-2- pyridine	2-MeO-phenyl	NB	-	-	
	40	3,5-diCl-2- pyridine	2-MeO-phenyl	NB	-	-	
	Nivolumab						6.7 ± 2.7
NB	BMS-202				37±9	124 ± 12	= No

binding; Data are mean ± SEM of three experiments performed in duplicate.

Isothermal Titration Calorimetry (ITC) assay.

To complete this study and to support the MST results, the affinity of compound **32** for PD-L1 was evaluated by Isothermal Titration Calorimetry (ITC). We selected compound **32** (obtained in a large quantity) as an example of potent PD-L1 binder (according to the above MST data) to confirm the PD-L1 interaction with an independent orthogonal method. Every interaction between two molecules generates or absorbs heat, depending on the thermodynamic nature of the interaction. This heat change can be measured by ITC. From the raw heat pulses, binding isotherms are derived that deliver comprehensive informations of the affinity, stoichiometry, and thermodynamics of molecular interactions.

The raw heat plot (Figure 10A) shows titration peaks with an overall signal spread of 0.3 µcal/s. The enthalpy plot (Figure 10B) indicates an interaction between compound **32** and PD-L1. The following binding parameters were obtained: a K_D (steady state affinity) = 177 ± 93 nM, N (reaction stoichiometry) = 0.97 ± 0.09 (indicating 1:1 interaction), ΔG (free enthalpy of binding) = -0.922 kcal/mol (indicating exergonic reaction). These ITC data thus support and validate the MST data.

A)

B)

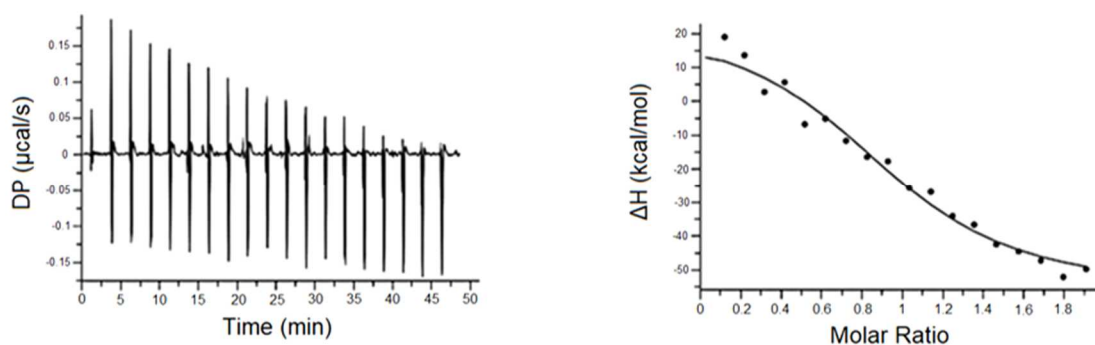


Figure 10. Results of the ITC experiments performed with compound **32**. (A) The titration of raw data between differential power (DP, $\mu\text{cal/s}$) and time (min) after sequential injection of ligand ($12.4 \mu\text{M}$) into the protein solution ($1.24 \mu\text{M}$) was plotted. (B) The integrated heat after the correlation between enthalpy changes *versus* the molar ratios of compound **32** to protein (**rhPD-L1 Fc Chimera**) was plotted. Data were fitted using a one-site binding model where the solid lines represented the best-fit results

Binding mode of compound **17**.

The crystal structure of compound BMS-202 bound to PD-L1 (PDB code 5J89) has provided a detailed knowledge of the mode of binding of this reference compound to the dimeric protein junction. We selected one of our good compounds (**17**) to perform a docking study to the PD-L1 dimer (using the procedure outlined in other PD-L1 docking studies [37]). MST dimerization binding assay (Table 1) and our computational analysis indicated that compound **17** can bind to the PD-L1 dimer interface as observed with **BMS-202**.

The binding mode of pyrazolone compound is comparable to that of the BMS compounds, at the junction of two PD-L1 unit. The molecule was stabilized into the interfacial pocket defined by the key tyrosine residues Y56 (chain A), Y123(A), Y56(B) and Y123(B) (Figure 11). Compound **17** remains solidly anchored to the PD-L1 dimer, establishing numerous contacts with the two protein subunits. Up to 12 different interactions were observed, including van der Waals contacts, H-bonds, π - π stacking, π -alkyl and π -sulfur interactions (Figure 11).

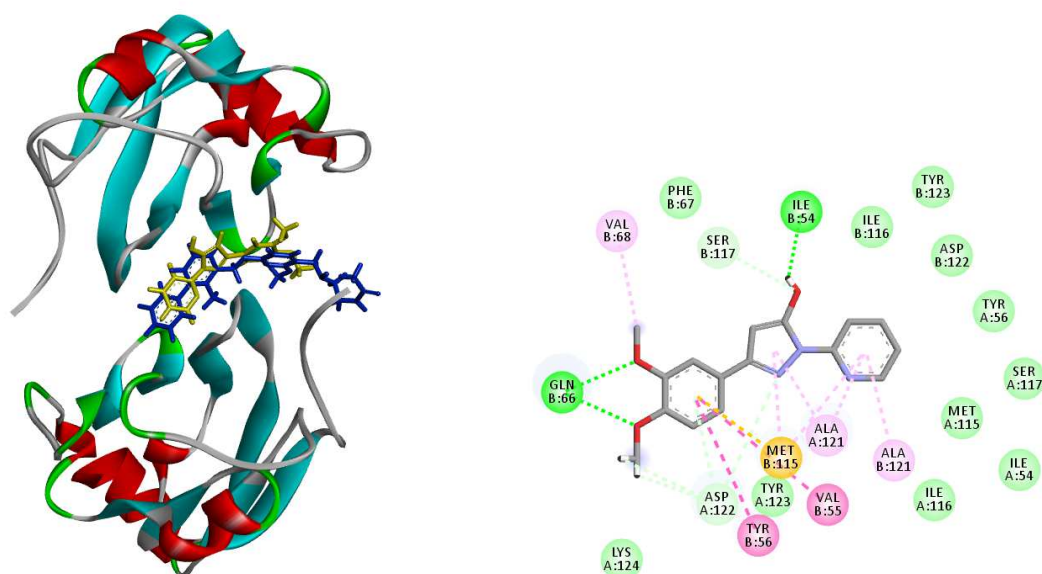


Figure 11. Interactions observed between compound **17** (yellow) or **BMS-202** (blue) and the PD-L1 dimer. Compound **17** stabilizes the PD-L1 dimer and fits into a pocket defined by the key tyrosine residues Y56 (chain A), Y123(A), Y56(B) and Y123(B) of the PD-L1 dimer.

The stability of the receptor-ligand complex was evaluated through the empirical potential energy of interaction as defined above. The Molecular Mechanics/Generalized Born Surface Area (MM/GBSA) procedure was used to evaluate free energies of hydration [38] within the BOSS/MCPRO program, in relation with aqueous solubility [39]. The calculated binding energy (ΔE) for the drug bound to the protein dimeric model is -56.45 kcal/mol (and the free energy of hydration ΔG is -17.80 kcal/mol) *versus* -74.90 kcal/mol (and the free energy of hydration ΔG is -20.50 kcal/mol) for BMS-202 in the corresponding complex.

PD-L1 ligand-induced reactivation of CTLL-2 cells

To mimic the rescue of a T-cell response, we used CTLL-2 cells expressing CD-80 (B7-1), and dormant when they were exposed to recombinant *h*PD-L1. In this cell-based assay, the proliferation of the cells is investigated by flow cytometry (Figure 12) and CyQuant cell proliferation kit (Thermofischer). The addition of a PD-L1 inhibitor reactivates CTLL-2 cells proliferation mimicking a reactivation of the immune system [40-41].

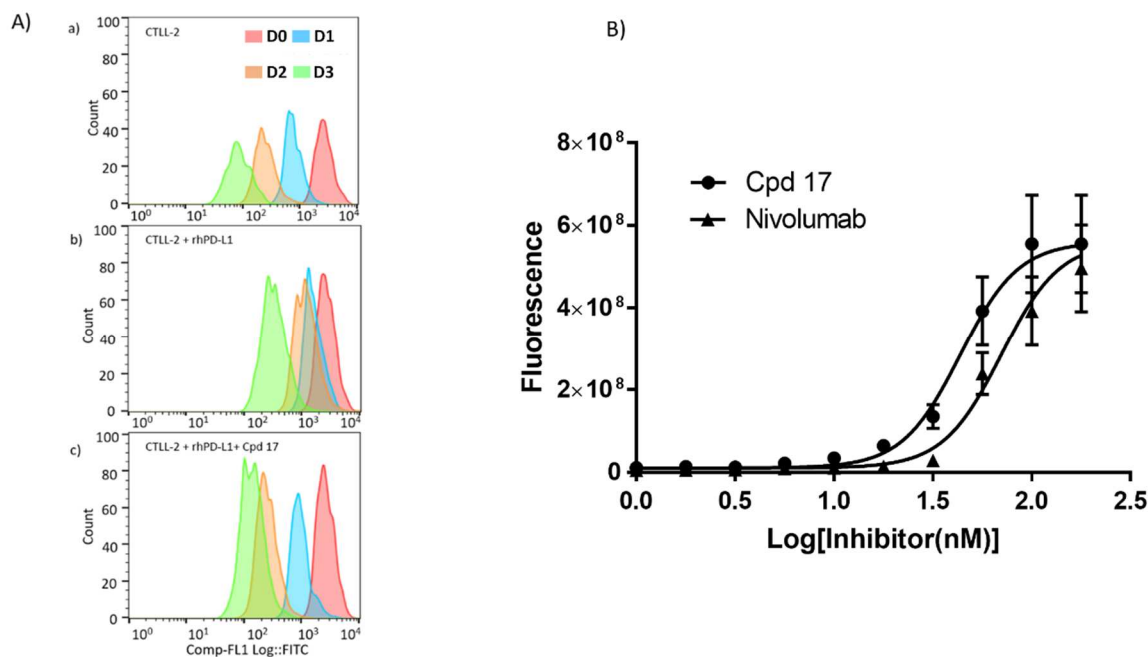


Figure 12. Results of CTLL-2 cells proliferation test with compound **17**. (A) CTLL-2 proliferation by flow cytometry alone (a), with recombinant *rhPD-L1* (b) and with recombinant *hPD-L1* and compound **17** (c). A fluorescent dye (CFSE) was used to monitor cell proliferation using flow cytometry. In the control (a) the number of fluorescent CTLL-2 cells decreases at each cell generation. With *rhPD-L1* (b) the proliferation is delayed and then restored in the presence of compound **17**(c). (B) Effect of two compounds on growth binding curve: IC₅₀ of compound **17** (4.1 ± 1.2 nM) vs nivolumab (58 ± 3 nM) using CyQuant cell proliferation kit on CTLL-2 cells. IC₅₀ value of BMS-202 = 53 ± 17 nM.

Our best selected compounds (**3**, **11**, **17**, **22** and **32**; IC₅₀ (FRET) < 100 nM) display 10-100 nM IC₅₀ in this proliferation test (4.1 ± 1.2 nM for the best compound, vs. 58 ± 3 nM with nivolumab, Table 2). They do not present direct cytotoxic properties toward cancer cells (IC₅₀ > 1 μM, data not shown).

Solubility, logD and plasma stability on mouse CD-1 plasma measurements.

The best compounds were selected for a preliminary ADME study (Table 2). We have evaluated solubility, lipophilicity (logD) and stability of compounds on mouse CD-1 plasma. Results indicated a poor solubility (1.9 μM) and a high lipophilicity (logD = 4,277) for the adamantane compound **32**. For the other compounds the solubility and lipophilicity data were in agreement with our selection criteria (solubility > 80.9 μM and 0.8 < logD < 2,82). However, all prepared pyrazolones were found to be unstable in mouse plasma (t_{1/2} < 30 min). The plasma stability must be improved in future drug design.

Table 2. Reactivation of CTLL-2 cells proliferation and ADME properties of selected compounds.

Compounds	R ₁	R ₂	IC ₅₀ (nM) CyQuant Cell proliferation	ADME properties solubility, logD, t _{1/2} (stability on of male mice plasma)
3	2-pyridine	2-MeO-phenyl	14 ± 4	solubility = 80.9 μM logD = 2.56 t _{1/2} (plasma) = 10.9 min
11	2-pyridine	4-MeO-phenyl	75 ± 4	solubility = 199.2 μM logD = 2.82 t _{1/2} (plasma) = 12 min
17	2-pyridine	3,4-diMeO-phenyl	4.1 ± 1.2	solubility = 183 μM logD = 2.19 t _{1/2} (plasma) = 30 min
22	2-pyridine	Methyl	102 ± 8	solubility > 200 μM logD = 0.85 t _{1/2} (plasma) = 16 min
32	2,4-diCl-phenyl	Adamantane	54 ± 3	solubility = 1.9 μM logD = 4.28 t _{1/2} (plasma) = 31 min
Nivolumab			58 ± 3	

Data (IC₅₀) are mean ± SEM of three experiments performed in duplicate; ND = Not determined.

CONCLUSION

A series of compounds was designed around the pyrazolone scaffold. Thirty-nine new molecules have been synthesized, leading to the discovery of 5 original compounds as immune checkpoint inhibitors blocking PD-1/PD-L1 interactions in the nanomolar range. Pharmacomodulations were carried out and pointed out to the 2-pyridine group as a pharmacophoric element for PD-L1 recognition. Our best compounds were able to disrupt the PD-1/PD-L1 interaction and to reactivate CTLL-2 cells proliferation. These compounds represent a new promising series for the design of PD-L1 ligands. However, further structural optimizations will be required to improve the stability of the compounds in murine plasma, a prerequisite for *in vivo* testing. Further drug design is on-going in our laboratories. In recent years, diverse series of small molecules targeting the PD-1/PD-L1 checkpoint have been reported [19]. Many of these small molecules bears a biphenyl core (as the BMS ligands) or another biaromatic system. To our knowledge, the phenyl-pyrazolone core is used here for the first time. This ring system can be found in a few clinically useful compounds (such as edaravone). Interesting development in this series are anticipated.

EXPERIMENTAL SECTION

MicroScale Thermophoresis (MST). MST was conducted using a NT.115 Pico MST instrument (Nano Temper Technologies GmbH) equipped with red and blue filter sets. His-PD-L1 protein (Biotechne # 9049-B7-100), was diluted to 200 nM in PBS-T buffer (supplied by vendor) was labeled with Monolith His-Tag Labeling Kit RED-tris-NTA (Nano Temper). The RED-tris-NTA dye was diluted in PBS-T to 100 nM [42]. The mix was incubated at room temperature in the dark for 30 min. Ligands (50 μ M) were diluted with a serial 1:1 ratio of 16 gradients. Then the labeled protein and ligands were mix with 1:1 ratio and incubated at room temperature in the dark for 15 min. Capillaries are then filled individually and loaded into instrument. Data were acquired using medium MST power and 20 % LED. Data were analyzed using MO Control Software (Nano Temper). MST figures were rendered using MO Affinity Analysis (Nano Temper).

MST Dimerization Binding Assay. BMS-202 and five of our best compounds have been tested using a different approach of the MST experiment. A labelled His-PD-L1 protein was titrated against an unlabeled His-PD-L1 protein with or without compounds of interest. The concentration of the compound under study (1 μ M) and the His-labelled PD-L1 protein (10 nM) are kept constant whereas the unlabeled His-PD-L1 (1 μ M) varies with a serial 1:1 ratio of 16 gradients. MST was conducted using a NT.115 Pico MST instrument (Nano Temper Technologies GmbH) equipped with red and blue filter sets. His-PD-L1 protein (Biotechne # 9049-B7-100), was diluted to 200 nM in PBS-T buffer (supplied by vendor) was labeled with Monolith His-Tag Labeling Kit RED-tris-NTA (Nano Temper). The RED-tris-NTA dye was diluted in PBS-T to 100 nM. The mix was incubated at room temperature in the dark for 30 min. Capillaries are then filled individually and loaded into instrument. Data were acquired using medium MST power and 20 % LED. Data were analyzed using MO Control Software (Nano Temper).

Fluorescence Resonance Energy Transfer (FRET) assay. A model was developed using CHO-K1 cells involving overexpression of proteins of interest. It involves the expression of a PD-1-YFP fluorescent protein and a second fluorescent protein SHP-2-CFP (phosphatase recruited during the interaction between PD-1 and PD-L1). During excitation at a given length (λ CFP 445-485 nm, λ YFP 485-535 nm), an energy transfer takes place when the proximity is sufficient between the two proteins resulting in a FRET phenomenon. Using a blocking

compound, the interaction is inhibited. Therefore, the recruitment of phosphatase no longer intervenes. The FRET phenomenon is therefore no longer observed.

A Spectramax i3 (Molecular Devices) is configured according to the selected fluorochromes with their excitation and emission spectra. Endpoint reading is performed, at the center of the well; the reading time is 2 minutes for a 96-well plate. For this testing, a 96-well flat-bottomed white plate is required. All mixes introduced into the plate are made of triplicate. The negative control is provided by the CHO transfected by the void plasmid, the positive control is provided by CHO transfected with a plasmid containing the YFP-CFP fusion protein making it possible to mimic the FRET phenomenon. To check that the two fluorochromes do not emit in the FRET channel separately, the PD1-YFP and SHP2-CFP constructs are checked separately. It is also necessary to remove the background noise, that is to say the FRET without activation with PD-L1. After the addition of rhB7-H1 (10 μ M) to our co-transfected PD1-SHP2 cells, dose-response curves are performed to determine the IC₅₀ of the molecule under study. The IC₅₀ values are obtained using Graphpad and the results are listed above. Nivolumab was taken as positive control of interaction's inhibitions.

Isothermal Titration Calorimetry (ITC). ITC was performed by a CRO according to 2bind protocol (2bind molecular interactions, Regensburg, Germany). All samples were stored at -80°C prior to experiments. To prepare samples, the stock solution of the test compound (20 mM in DMSO) was diluted to achieve the desired final concentration while maintaining the required buffer condition (PBS). A stock solution of the protein (20 μ M) was prepared using the same buffer. The final ligand assay solution was filled into the titration syringe of the ITC device. The experiments were performed on a Malvern PEAQ-ITC device. Data were analyzed using the corresponding PEAQ-ITC Analysis Software.

In Silico Molecular Docking Procedure. The model used to investigate the docking study of compounds refers to the crystallographic structure (PDB code 5J89) of a smaller fragment of PD-L1 stabilized as a dimer by BMS-202 (X-ray diffraction at 2.2 Å resolution) [43]. The drug fits into a narrow cavity at the interface of two PD-L1 molecules [44-45]. Docking experiments were performed with the GOLD software (GOLD 5.3 release, Cambridge Crystallographic Data Centre, Cambridge, UK). Before starting the docking procedure, the structure of the ligand has been optimized using a classical Monte Carlo conformational searching procedure as described in the BOSS/MCPRO software [46]. Based on shape complementarity criteria, the only possible binding site has been defined around Y56 and

Y123 residues of each PD-L1 unit. Shape complementarity and geometry considerations are in favor of a docking grid centered in the volume defined by Y56 (chain A), Y123 (A), Y56 (B) and Y123 (B). Within the binding site, side chains of following amino acids have been considered as fully flexible: Y56 (A and B), Y123 (A and B), M115 (A and B), D122 (A and B), K124 (A) and Q66 (B). The ligand is defined as flexible during the docking procedure. Up to 100 poses that are energetically reasonable were kept while searching for the correct binding mode of the ligand. The decision to keep a trial pose is based on ranked poses, using the PLP fitness scoring function (which is the default in GOLD version 5.3 used here [47]). In addition, an empirical potential energy of interaction ΔE for the ranked complexes is evaluated using the simple expression $\Delta E(\text{interaction}) = E(\text{complex}) - (E(\text{protein}) + E(\text{ligand}))$. For that purpose, the Spectroscopic Empirical Potential Energy function SPASIBA and the corresponding parameters were used [48]. Molecular graphics and analysis were performed using Discovery Studio Visualizer, Biovia 2020 (Dassault Systèmes BIOVIA Discovery Studio Visualizer 2020, San Diego, Dassault Systèmes, 2020).

CFSE Cell Proliferation Kit, for flow cytometry and CyQUANT cell proliferation kit (Thermofischer). CellTrace CFSE (Invitrogen) kit is used to monitor distinct generations of proliferating cells by dye dilution. CTLL-2 cells (ATCC) are covalently labeled with a very bright, stable dye. Every generation of cells appears as a different peak on a flow cytometry histogram. Experiment is performed over three days. CTLL-2 cells [49] are exposed to exogen rhB7-H1 Fc Chimera (R&D). Measurements were performed on individual dilution series with each compound. A positive control (Nivolumab) and negative control (no rhB7-H1 Fc Chimera) were also evaluated. CyQUANT was used to evaluate the growth of CTLL-2 cell line. Cells were prepared for the CyQUANT assay by growing them in presence or absence of rhB7-H1 plus compounds then transferred to microplates for assay according to manufacturer's instructions (Molecular Probes C35011). A cell based standard curve was first performed. Then, since the amount of fluorescence is correlated to the quantity of cells in wells, we determined and IC_{50} for the restoration of proliferation with various concentrations of compounds resulting in a IC_{50} by global fitting with Graphpad using final proliferation after 72h. Experiments was performed over 3 days and was repeated three times.

LC-MS/MS ADME Methods. Chromatography was performed using a UPLC system, an Acquity I-Class (Waters). Separation was achieved on a Waters Acquity BEH C18 column (2.1 mm \times 50 mm, 1.7 μ m). The autosampler and column oven temperatures were 10 and 40

°C, respectively, and the sample injection volume was 1 μ L. The mobile phase consisted of 0.1% formic acid in water as solvent A and 0.1% formic acid in acetonitrile as solvent B at a flow rate of 600 μ L/min. The gradient was as follows: 0–0.2 min (98%A and 2%B), 2–2.5 min (2%A and 98%B), 2.6 min (98%A and 2%B), 4 min (98% A and 2%B). The gradient step was linear. Mass spectrometry was performed using a Xevo TQD (Waters Corporation) mass spectrometer. The detection of analytes was achieved by electrospray ionization (ESI) in the positive mode with the appropriate MRM transition. For polydisperse PEGylated compounds, LC-MS analyses were performed using several transitions of several of the most abundant species in the mixture. Other mass spectrometer settings were as follows: capillary voltage and cone voltage were optimized for each compound, desolvation temperature 600 °C at a gas flow of 1200 L/h and cone gas flow 50 L/h. The LC-MS/MS instrument was controlled by MassLynx software (Waters).

Solubility Measurements. Ten microliters of a 10 mM solution in DMSO of the compound was diluted either in 490 μ L of PBS pH 7.4 or in organic solvent MeOH in a PP tube (n = 3 for PBS, n = 6 for MeOH). The tubes were gently shaken for 24 h at room temperature. Then, PBS tubes and three of the six methanol tubes were centrifuged for 5 min at 4000 rpm and filtered over 0.45 μ m filters (Millex-LH Millipore). Then, 10 μ L of each sample was diluted in 490 μ L of MeOH before LC-MS analysis. The solubility is determined by the ratio of mass signal area PBS/organic solvent.

LogD Measurements. Forty microliters of a 10 mM solution in DMSO of the compound was diluted in 1.960 mL of a 1/1 octanol/PBS at pH 7.4 mixture. The mixture was gently shaken for 2h at room temperature. Ten microliters of each phase were diluted in 490 μ L of MeOH and analyzed by LC-MS/MS. Each compound was tested in triplicate. LogD was determined as the logarithm of the ratio of concentration of product in octanol and PBS, respectively, determined by mass signals.

Plasma stability on Mouse CD-1 Plasma. The products tested and the reference (enalapril) are incubated in duplicate at 37°C in mouse CD-1 plasma (plasma pre-incubated 10 min before addition of the compound), at a final concentration of 10 μ M (0.1% DMSO). In order to calculate half-life, aliquots are taken at 0, 15, 30, 60, 130, 240 and 360 min and transferred to tubes containing ice-cold acetonitrile + internal standard. After being vigorously agitated, the samples are centrifuged 10 min at 12000 rpm, 4°C; the supernatants are transferred into

Matrix tubes and maintained at 4°C for immediate analysis (or placed at -80°C if the analysis is postponed).

Chemistry. Analytical thin-layer chromatography was performed on precoated Kieselgel 60F₂₅₄ plates (Merck); the spots were located by UV (254 nm). Silica gel 60 230-400 mesh purchased from Merck was used for column chromatography. Preparative thick-layer chromatography (TLC) was performed using silica gel from Merck. Ultrasound protocols were carried out in an ultrasonic cleaning bath (Elma, Model: D-78224 Singen/Htw, Germany; overall dimensions: 340 × 300 × 370 mm; internal dimensions: 240 × 130 × 150 mm) with temperature and time control. The bath was operated at frequency of 35 kHz. The microwave reactions were performed using a CEM DiscoverSP, in sealed reaction vials, and the temperature was monitored using IR temperature sensor. All melting points were determined with a Büchi 535 capillary apparatus and remained uncorrected. Nuclear magnetic resonance (¹H and ¹³C NMR) spectra were recorded at room temperature on a Bruker AC 300 spectrometer. Tetramethylsilane (TMS) was used as an internal standard and CDCl₃ or DMSO-*d*₆ as the solvents. ¹H NMR analyses were obtained at 300 MHz (s: singlet, d: doublet, t: triplet, q: quadruplet, quint.: quintuplet, sext.: sextuplet, hept.: heptuplet, dd: double doublet, m: multiplet); whereas ¹³C NMR analyses were obtained at 75.4 MHz. The chemical shifts (δ) are given in parts per million (ppm) relative to TMS (δ = 0.00). All compounds were analyzed by LC-MS on a HPLC combined with a Surveyor MSQ (Thermo Electron) equipped with an APCI-source. All tested compounds showed purity higher than 96% in APCI⁺ mode. A Micromass (Waters, Manchester, UK) high resolution TOFMS with an ESI source was used to detect the analytes of interest in positive mode or negative mode. The TOF analyser was used in V mode at 9000 mass resolution.

General procedure for preparation of β-keto esters (1a-c) from ketone derivatives.

NaH (60% in dispersion in oil, 4 eq.) was mixed in anhydrous toluene (0.8 M) under inert atmosphere. Diethylcarbonate (3 eq.) was added and the reaction mixture was brought to reflux for 1h. The corresponding ketone (1 eq.), diluted in anhydrous toluene (1.6 M), was then added dropwise in the mixture. After the addition, the mixture was kept to reflux until no dihydrogene gas was generated anymore (30 minutes – 1 hour). The mixture was gradually cooled to 0°C and then acetic acid (0.3 M) was added dropwise. Ice water was added until the formed solid was dissolved. The toluene layer was separated and the water layer was

extracted three times with EtOAc. The combined organic layers were then washed with water, brine, then dried over MgSO₄. The solvent was evaporated under reduced pressure.

Ethyl 3-(4-chloro-2-methoxyphenyl)-3-oxopropanoate (1a).

The product was purified by flash chromatography (cyclohexane/AcOEt 1:0 → 9:1). A yellow oil was obtained: yield 40% (560 mg). ¹H NMR (CDCl₃) δ 7.86 (d, 1H, *J* = 8.4 Hz); 7.05 (dd, 1H, *J* = 8.4, 1.8 Hz); 6.98 (dd, 1H, *J* = 1.8 Hz); 4.19 (q, 2H, *J* = 7.6 Hz); 3.96 (s, 2H); 3.92 (s, 3H); 1.25 (t, 3H, *J* = 7.6 Hz), LC-MS (ESI) *m/z* 257 (MH⁺), *t_r* 2.87 min, λ_{max} 255 nm.

Ethyl 3-oxo-3-(pyridin-2-yl)propanoate (1b).

The product was purified by flash chromatography (cyclohexane/AcOEt 1:0 → 9:1). A red oil was obtained: yield 33% (1.02 g). ¹H NMR (CDCl₃) δ 8.68 (ddd, 1H, *J* = 5.1, 1.5, 0.9 Hz); 8.09 (ddd, 1H, *J* = 8.9, 1.1, 0.9 Hz); 7.86 (ddd, 1H, *J* = 8.9, 7.3, 1.6 Hz); 7.50 (ddd, 1H, *J* = 7.3, 5.1, 1.1 Hz); 4.20 (m, 4H); 1.37 (t, 3H, *J* = 7.1 Hz), LC-MS (ESI) *m/z* 194 (MH⁺), *t_r* 2.25 min, λ_{max} 235 nm.

Ethyl 3-oxo-3-(p-tolyl)propanoate (1c).

The product was purified by flash chromatography (cyclohexane/AcOEt 1:0 → 9:1). An orange oil was obtained: yield 66% (2.03 g). ¹H NMR (CDCl₃) δ 7.88 (d, 2H, *J* = 8.2 Hz); 7.30 (d, 2H, *J* = 8.2 Hz); 4.25 (q, 2H, *J* = 7.3 Hz); 3.98 (s, 2H); 2.43 (s, 3H); 1.25 (t, 3H, *J* = 7.3 Hz), LC-MS (ESI) *m/z* 207 (MH⁺), *t_r* 2.74 min, λ_{max} 251 nm.

General procedure for preparation of β-keto esters (1d-e) from acyl chloride derivatives.

Potassium ethyl malonate (2.1 eq.) was mixed in anhydrous acetonitrile (0.8 M) under inert atmosphere. The mixture was stirred and cooled down to 0°C. Et₃N (3 eq.) was added followed by magnesium chloride (2.5 eq.), and stirring continued for 2.5 hours. The mixture was cooled down to 0°C and the corresponding acyl chloride (1 eq.) diluted in anhydrous acetonitrile (0.4 M) was added dropwise. The mixture was then stirred overnight at room temperature after adding 0.25 eq of Et₃N. The solvent was then evaporated under reduced pressure. Toluene was added and the mixture was cooled to 0°C. Aqueous HCl (13%) was added dropwise, the organic layer was separated and extracted with aqueous HCl (13%) two times followed by H₂O two times, dried over MgSO₄ and concentrated under reduced pressure.

Ethyl 3-oxo-3-(o-tolyl)propanoate (1d).

The product was purified by flash chromatography (cyclohexane/AcOEt 1:0 → 9:1). An orange oil was obtained: yield 95% (1.30 g). ¹H NMR (CDCl₃) δ 7.68 (m, 1H); 7.43 (m, 1H); 7.32 (m, 2H); 4.22 (q, 2H, *J* = 7.2 Hz); 3.97 (s, 2H); 2.57 (s, 3H); 1.26 (t, 3H, *J* = 7.2 Hz), LC-MS (ESI) *m/z* 207 (MH⁺), *t_r* 2.75 min, λ_{max} 239 nm.

Ethyl 3-(3-chlorophenyl)-3-oxopropanoate (1e).

The product was purified by flash chromatography (cyclohexane/AcOEt 1:0 → 9:1). An orange oil was obtained: yield 95% (1.35 g). ¹H NMR (CDCl₃) δ 7.91 (s, 1H); 7.80 (d, 1H, *J* = 7.9 Hz); 7.55 (d, 1H, *J* = 7.2 Hz); 7.41 (m, 1H); 4.22 (q, 2H, *J* = 7.2 Hz); 3.97 (s, 2H); 1.26 (t, 3H, *J* = 7.2 Hz), LC-MS (ESI) *m/z* 227 (MH⁺), *t_r* 2.81 min, λ_{max} 250 nm.

Ethyl 3-oxo-3-(m-tolyl)propanoate (1f).

Carboxylic acid derivative (1 eq.) was mixed in anhydrous dichloromethane (0.7M) under inert atmosphere. 4-Dimethylaminopyridine (2 eq.), Meldrum's acid (1.2 eq.), dicyclohexylcarbodiimide (1.1 eq.) were then added at 0°C. The reaction was stirred at room temperature for 2 hours. The obtained solid was filtered and washed with dichloromethane. The filtrate was concentrated under reduced pressure and the mixture was dissolved in absolute EtOH (0.15 M). *p*-TSA (2.5 eq.), diluted in absolute EtOH (2 M), was then added. The mixture was refluxed for about one hour. The solvent was evaporated under reduced pressure and dissolved in EtOAc. The organic extract was then washed with H₂O, aq. sat. NaHCO₃, aq. HCl (10%), brine and dried over MgSO₄. The solvent was evaporated under reduced pressure. The product was purified by flash chromatography (cyclohexane/AcOEt 1:0 → 9:1). An orange oil was obtained: yield 95% (1.35 g). ¹H NMR (CDCl₃) δ 7.78 (m, 2H); 7.39 (m, 2H); 4.22 (q, 2H, *J* = 7.2 Hz); 3.99 (s, 2H); 2.43 (s, 3H); 1.26 (t, 3H, *J* = 7.2 Hz), LC-MS (ESI) *m/z* 207 (MH⁺), *t_r* 2.75 min, λ_{max} 252 nm.

General procedure of preparation of non-alkylated pyrazolones (2-21 and 28-40)

The corresponding β-keto ester (1 eq.) and hydrazine (1.5 eq.) were dissolved in glacial acetic acid (6M). The mixture was sonicated until precipitation of the desired product or complete conversion. The reaction was followed by TLC. The eventual precipitate was then collected and the acetic acid was evaporated under reduced pressure.

3-Phenyl-1-(pyridin-2-yl)-1H-pyrazol-5-ol (2). The formed precipitate was filtered and washed with ethanol (Fraction 1: 420 mg). The filtrate was concentrated under reduced

pressure, diluted with ethyl acetate and purified by flash chromatography (cyclohexane/AcOEt 1:0 → 8:2) (Fraction 2: 280 mg). Two fractions of light yellow powder were obtained: yield 85% (700 mg); mp $118 \pm 1^\circ\text{C}$; $^1\text{H NMR}$ (CDCl_3) δ 12.79 (br, 1H); 8.29 (ddd, 1H, $J = 5.1, 1.5, 0.9$ Hz); 8.08 (ddd, 1H, $J = 8.3, 1.1, 0.9$ Hz); 7.90 (m, 3H); 7.38 (m, 3H); 7.18 (ddd, 1H, $J = 7.3, 5.1, 1.1$); 5.86 (s, 1H); $^{13}\text{C NMR}$ (CDCl_3) δ 157 (C^{IV}); 154 (C^{IV}); 152 (C^{IV}); 145 (CH); 139 (CH); 133 (C^{IV}); 128.6 (2CH); 128.5 (CH); 125 (2CH); 119 (CH); 112 (CH); 86 (CH); LC-MS (ESI) m/z 238 (MH^+), t_r 3.10 min, λ_{max} 262 nm; HRMS (ESI-TOF) m/z $[\text{M}+\text{H}]^+$ calcd for $\text{C}_{14}\text{H}_{12}\text{N}_3\text{O}$ 238.0975, found 238.0976.

3-(2-Methoxyphenyl)-1-(pyridin-2-yl)-1H-pyrazol-5-ol (3). The solvent was removed under reduced pressure. The solid obtained was purified by flash chromatography (cyclohexane/AcOEt 1:0 → 5:5). A light yellow powder was obtained: yield 82% (170 mg); mp $134 \pm 1^\circ\text{C}$; $^1\text{H NMR}$ (CDCl_3) δ 12.71 (br, 1H); 8.29 (ddd, 1H, $J = 5.1, 1.5, 0.9$ Hz); 8.06 (m, 2H); 7.99 (ddd, 1H, $J = 8.3, 1.1, 0.9$ Hz); 7.36 (ddd, 1H, $J = 8.7, 7.7, 0.8$ Hz); 7.18 (ddd, 1H, $J = 7.3, 5.1, 1.1$ Hz); 7.07 (td, 1H, $J = 7.7, 0.8$ Hz); 7.00 (dd, 1H, $J = 8.7, 0.8$); 6.22 (s, 1H); 3.94 (s, 3H); $^{13}\text{C NMR}$ (CDCl_3) δ 157 (C^{IV}); 156 (C^{IV}); 154 (C^{IV}); 150 (C^{IV}); 145 (CH); 140 (CH); 130 (CH); 129 (CH); 121 (CH); 120 (CH); 119 (C^{IV}); 112 (CH); 90 (CH); 55 (CH_3); LC-MS (ESI) m/z 268 (MH^+), t_r 2.84 min, λ_{max} 303 nm; HRMS (ESI-TOF) m/z $[\text{M}+\text{H}]^+$ calcd for $\text{C}_{15}\text{H}_{14}\text{N}_3\text{O}_2$ 268.1081, found 268.1079.

3-(2-Chlorophenyl)-1-(pyridin-2-yl)-1H-pyrazol-5-ol (4). The solvent was removed under reduced pressure. The solid obtained was purified by flash chromatography (cyclohexane/AcOEt 1:0 → 5:5). A white yellow powder was obtained: yield 85% (350 mg); mp $103 \pm 1^\circ\text{C}$; $^1\text{H NMR}$ (CDCl_3) δ 12.73 (br, 1H); 8.30 (ddd, 1H, $J = 5.1, 1.5, 0.9$ Hz); 8.02 (ddd, 1H, $J = 8.3, 1.1, 0.9$ Hz); 7.85 (m, 2H); 7.46 (m, 1H); 7.32 (m, 2H); 7.18 (ddd, 1H, $J = 7.3, 5.1, 1.1$ Hz); 6.13 (s, 1H); $^{13}\text{C NMR}$ (CDCl_3) δ 157 (C^{IV}); 154 (C^{IV}); 151 (C^{IV}); 145 (CH); 140 (CH); 132.7 (C^{IV}); 132.3 (C^{IV}); 130.5 (CH); 130.4 (CH); 129 (CH); 127 (CH); 120 (CH); 112 (CH); 89 (CH); LC-MS (ESI) m/z 272 (MH^+), t_r 3.32 min, λ_{max} 210 nm; HRMS (ESI-TOF) m/z $[\text{M}+\text{H}]^+$ calcd for $\text{C}_{14}\text{H}_9\text{ClN}_3\text{O}$ 270.0429, found 270.0434.

1-(Pyridin-2-yl)-3-(o-tolyl)-1H-pyrazol-5-ol (5). The solvent was removed under reduced pressure. The solid obtained was purified by flash chromatography (cyclohexane/AcOEt 1:0 → 5:5). A white yellow powder was obtained: yield 14% (45 mg); mp $154 \pm 1^\circ\text{C}$; $^1\text{H NMR}$ (CDCl_3) δ 12.64 (br, 1H); 8.30 (ddd, 1H, $J = 5.1, 1.5, 0.9$ Hz); 8.04 (ddd, 1H, $J = 8.3, 1.1, 0.9$ Hz); 7.89 (ddd, 1H, $J = 8.3, 1.1, 0.9$ Hz); 7.64 (m, 1H); 7.31 (m, 3H); 7.18 (ddd, 1H, $J = 7.3,$

5.1, 1.1 Hz); 5.86 (s, 1H); 2.60 (s, 3H); ^{13}C NMR (CDCl_3) 157 (C^{IV}); 154 (C^{IV}); 153 (C^{IV}); 145 (CH); 140 (CH); 136 (C^{IV}); 133 (C^{IV}); 131 (CH); 129 (CH); 128 (CH); 126 (CH); 119 (CH); 111 (CH); 89 (CH); 21 (CH_3); LC-MS (ESI) m/z 252 (MH^+), t_r 3.22 min, λ_{max} 210 nm; HRMS (ESI-TOF) m/z $[\text{M}+\text{H}]^+$ calcd for $\text{C}_{15}\text{H}_{14}\text{N}_3\text{O}$ 252.1131, found 252.1131.

3-(2-Fluorophenyl)-1-(pyridin-2-yl)-1H-pyrazol-5-ol (6). The solvent was removed under reduced pressure. The solid obtained was recrystallized in ethanol and filtered (Fraction 1: 500 mg). The filtrate was concentrated under reduced pressure and purified by flash chromatography (cyclohexane/AcOEt 1:0 \rightarrow 5:5) (Fraction 2: 150 mg). Two fractions of light yellow powder were obtained: yield 85% (650 mg); mp $98 \pm 1^\circ\text{C}$; ^1H NMR (CDCl_3) δ 12.79 (br, 1H); 8.29 (ddd, 1H, $J = 5.1, 1.5, 0.9$ Hz); 8.05 (ddd, 1H, $J = 8.9, 1.1, 0.9$ Hz); 7.93 (ddd, 1H, $J = 8.9, 7.3, 1.6$ Hz); 7.18 (ddd, 1H, $J = 7.3, 5.1, 1.1$ Hz); 5.99 (s, 1H); ^{13}C NMR (CDCl_3) δ 162-159 (d, $J_{\text{CF}} = 250$ Hz, C^{IV}); 157 (d, $J_{\text{CF}} = 2$ Hz, C^{IV}); 154 (C^{IV}); 148 (C^{IV}); 145 (CH); 140 (CH); 130 (d, $J_{\text{CF}} = 8$ Hz, CH); 128 (d, $J_{\text{CF}} = 3$ Hz, CH); 124 (d, $J_{\text{CF}} = 3$ Hz, CH); 121 (d, $J_{\text{CF}} = 11$ Hz, C^{IV}); 120 (CH); 116 (d, $J_{\text{CF}} = 22$ Hz, CH); 112 (CH); 89 (d, $J_{\text{CF}} = 10$ Hz, CH); LC-MS (ESI) m/z 256 (MH^+), t_r 3.18 min, λ_{max} 289 nm; HRMS (ESI-TOF) m/z $[\text{M}+\text{H}]^+$ calcd for $\text{C}_{14}\text{H}_{11}\text{FN}_3\text{O}$ 256.0881, found 256.0884.

3-(3-Methoxyphenyl)-1-(pyridin-2-yl)-1H-pyrazol-5(4H)-one (7). The formed precipitate was filtered and washed with ethanol (Fraction 1: 400 mg). The filtrate was concentrated under reduced pressure, recrystallized in ethanol (Fraction 2: 300 mg). Two fractions of light yellow powder were obtained: yield 95% (700 mg); mp $128^\circ\text{C} \pm 1^\circ\text{C}$; ^1H NMR (CDCl_3) δ 12.83 (br, 1H); 8.30 (ddd, 1H, $J = 5.1, 1.5, 0.8$ Hz); 8.07 (ddd, 1H, $J = 8.6, 1.1, 0.8$ Hz); 7.94 (ddd, 1H, $J = 8.6, 7.5, 1.7$ Hz); 7.83 (m, 2H); 7.18 (ddd, 1H, $J = 7.5, 5.1, 1.1$ Hz); 6.98 (m, 2H); 5.91 (s, 1H); 3.88 (s, 3H); ^{13}C NMR (CDCl_3) δ 160 (C^{IV}); 157 (C^{IV}); 154 (C^{IV}); 152 (C^{IV}); 145 (CH); 140 (CH); 127 (CH_2); 119 (CH); 114 (CH_2); 112 (CH); 85 (CH); 55 (CH_3); LC-MS (ESI) m/z 268 (MH^+), t_r 3.01 min, λ_{max} 210 nm; HRMS (ESI-TOF) m/z $[\text{M}+\text{H}]^+$ calcd for $\text{C}_{15}\text{H}_{14}\text{N}_3\text{O}_2$ 268.1081, found 268.1081.

3-(3-Chlorophenyl)-1-(pyridin-2-yl)-1H-pyrazol-5-ol (8). The formed precipitate was filtered and washed with ethanol (Fraction 1: 110 mg). The filtrate was concentrated under reduced pressure, purified by flash chromatography (cyclohexane/AcOEt 1:0 \rightarrow 8:2) (Fraction 2: 50 mg). Two fractions of light yellow powder were obtained: yield 77% (160 mg); mp $130^\circ\text{C} \pm 1^\circ\text{C}$; ^1H NMR (CDCl_3) δ 8.29 (ddd, 1H, $J = 5.1, 1.5, 0.9$ Hz); 8.06 (ddd, 1H, $J = 8.9, 1.1, 0.9$ Hz); 7.92 (ddd, 1H, $J = 8.9, 7.3, 1.6$ Hz); 7.88 (t, 1H, $J = 1.7$ Hz); 7.71

(dt, 1H, $J = 7.1, 1.7$); 7.34 (m, 2H); 7.20 (ddd, 1H, $J = 7.3, 5.1, 1.1$ Hz); 5.92 (s, 1H); ^{13}C NMR (CDCl_3) 157 (C^{IV}); 154 (C^{IV}); 151 (C^{IV}); 145 (CH); 140 (CH); 135 (C^{IV}); 134 (C^{IV}); 130 (CH); 128 (CH); 126 (CH); 124 (CH); 120 (CH); 112 (CH); 86 (CH); LC-MS (ESI) m/z 272 (MH^+), t_r 3.43 min, λ_{max} 293 nm; HRMS (ESI-TOF) m/z $[\text{M}-\text{H}]^-$ calcd for $\text{C}_{14}\text{H}_9\text{ClN}_3\text{O}$ 270.0429, found 270.0436.

1-(Pyridin-2-yl)-3-(m-tolyl)-1H-pyrazol-5-ol (9). The solvent was removed under reduced pressure. The solid obtained was recrystallized in ethanol and filtered (Fraction 1: 210 mg). The filtrate was concentrated under reduced pressure and purified by flash chromatography (cyclohexane/AcOEt 1:0 \rightarrow 5:5) (Fraction 2: 70 mg). Two fractions of light yellow powder were obtained: yield 60% (280 mg); mp $196 \pm 1^\circ\text{C}$; ^1H NMR (CDCl_3) δ 12.83 (br, 1H); 8.30 (ddd, 1H, $J = 5.1, 1.5, 0.9$ Hz); 8.09 (ddd, 1H, $J = 8.9, 1.1, 0.9$ Hz); 7.91 (ddd, 1H, $J = 8.9, 7.3, 1.6$ Hz); 7.73 (s, 1H); 7.67 (d, 1H, $J = 7.6$ Hz); 7.34 (t, 1H, $J = 7.6$ Hz); 7.19 (m, 2H); 5.96 (s, 1H); 2.45 (s, 3H); ^{13}C NMR (CDCl_3) δ 157 (C^{IV}); 154 (C^{IV}); 153 (C^{IV}); 145 (CH); 140 (CH); 138 (C^{IV}); 132 (C^{IV}); 129 (CH); 128 (CH); 126 (CH); 123 (CH); 119 (CH); 112 (CH); 85 (CH); 21 (CH_3); LC-MS (ESI) m/z 252 (MH^+), t_r 3.27 min, λ_{max} 295 nm; HRMS (ESI-TOF) m/z $[\text{M}+\text{H}]^+$ calcd for $\text{C}_{15}\text{H}_{14}\text{N}_3\text{O}$ 252.1131, found 252.1134.

1-(Pyridin-2-yl)-3-(3-(trifluoromethyl)phenyl)-1H-pyrazol-5-ol (10). The formed precipitate was filtered and washed with ethanol. A light yellow powder was obtained: yield 50% (370 mg); mp $108 \pm 1^\circ\text{C}$; ^1H NMR (CDCl_3) δ 12.87 (br, 1H); 8.29 (ddd, 1H, $J = 5.1, 1.5, 0.9$ Hz); 8.17 (s, 1H); 8.02 (d, 1H, $J = 7.7$ Hz); 7.95 (ddd, 1H, $J = 8.3, 1.1, 0.9$ Hz); 7.63 (d, 1H, $J = 7.7$ Hz); 7.56 (t, 1H, $J = 7.7$ Hz); 7.22 (ddd, 1H, $J = 7.3, 5.1, 1.1$ Hz); 5.99 (s, 1H); ^{13}C NMR (CDCl_3) δ 157 (C^{IV}); 154 (C^{IV}); 151 (C^{IV}); 145 (CH); 140 (CH); 134 (C^{IV}); 131 (q, $J_{\text{CF}} = 32$ Hz, C^{IV}); 129-119 (q, $J_{\text{CF}} = 273$ Hz, C^{IV}); 128 (2CH); 125 (q, $J_{\text{CF}} = 4$ Hz, CH); 123 (q, $J = 4$ Hz, CH); 120 (CH); 112 (CH); 86 (CH); LC-MS (ESI) m/z 306 (MH^+), t_r 3.49 min, λ_{max} 281 nm; HRMS (ESI-TOF) m/z $[\text{M}+\text{H}]^+$ calcd for $\text{C}_{15}\text{H}_{11}\text{F}_3\text{N}_3\text{O}$ 306.0849, found 306.0849.

3-(4-Methoxyphenyl)-1-(pyridin-2-yl)-1H-pyrazol-5-ol (11). The formed precipitate was filtered and washed with ethanol (Fraction 1: 140 mg). The filtrate was concentrated under reduced pressure, purified by flash chromatography (cyclohexane/AcOEt 1:0 \rightarrow 5:5) (Fraction 2: 300 mg). Two fractions of light grey powder were obtained: yield 75% (440 mg); mp $125 \pm 1^\circ\text{C}$; ^1H NMR (CDCl_3) δ 12.88 (br, 1H); 8.30 (ddd, 1H, $J = 5.1, 1.5, 0.9$ Hz); 8.08 (ddd, 1H, $J = 8.9, 1.1, 0.9$ Hz); 7.93 (ddd, 1H, $J = 8.9, 7.3, 1.6$ Hz); 7.84 (d, 2H, $J = 8.9$ Hz); 7.18 (ddd, 1H, $J = 7.3, 5.1, 1.1$ Hz); 7.00 (d, 2H, $J = 8.9$ Hz); 5.90 (s, 1H); 3.87 (s, 3H); ^{13}C

NMR (CDCl₃) δ 160 (C^{IV}); 157 (C^{IV}); 154 (C^{IV}); 152 (C^{IV}); 145 (CH); 140 (CH); 127 (2CH); 125 (C^{IV}); 128 (2CH); 127 (2CH); 114 (2CH); 112 (CH); 86 (CH); 55 (CH₃) LC-MS (ESI) m/z 268 (MH⁺), t_r 2.93 min, λ_{max} 288 nm; HRMS (ESI-TOF) m/z [M+H]⁺ calcd for C₁₅H₁₄N₃O₂ 268.1081, found 268.1079.

1-(Pyridin-2-yl)-3-(4-(trifluoromethyl)phenyl)-1H-pyrazol-5-ol (12). The formed precipitate was filtered and washed with ethanol. A yellow powder was obtained: yield 48% (33 mg); mp 142 \pm 1 °C; ¹H NMR (CDCl₃) δ 12.84 (br, 1H); 8.32 (ddd, 1H, J = 5.1, 1.5, 0.9 Hz); 8.08 (ddd, 1H, J = 8.9, 1.1, 0.9 Hz); 8.00 (m, 3H); 7.69 (d, 2H, J = 8.2 Hz); 7.23 (ddd, 1H, J = 7.3, 5.1, 1.1 Hz); 5.99 (s, 1H); ¹³C NMR (CDCl₃) δ 157 (C^{IV}); 154 (C^{IV}); 151 (C^{IV}); 145 (CH); 140 (CH); 136 (C^{IV}); 130 (q, J_{CF} = 32 Hz, C^{IV}); 126 (2CH); 125 (q, J_{CF} = 4 Hz, 2CH); 122 (q, J_{CF} = 270 Hz, 2CH); 120 (CH); 112 (CH); 86 (CH); LC-MS (ESI) m/z 306 (MH⁺), t_r 3.5 min, λ_{max} 294 nm; HRMS (ESI-TOF) m/z [M+H]⁺ calcd for C₁₅H₁₁F₃N₃O 306.0849, found 306.0852.

3-(4-Chlorophenyl)-1-(pyridin-2-yl)-1H-pyrazol-5-ol (13). The formed precipitate was filtered and washed with ethanol (Fraction 1: 270 mg). The filtrate was concentrated under reduced pressure, purified by flash chromatography (cyclohexane/AcOEt 1:0 \rightarrow 5:5) (Fraction 2: 170 mg). Two fractions of light grey powder were obtained: yield 95% (440 mg); mp 113 \pm 1 °C; ¹H NMR (CDCl₃) δ 12.83 (br, 1H); 8.29 (ddd, 1H, J = 5.1, 1.5, 0.9 Hz); 8.05 (ddd, 1H, J = 8.9, 1.1, 0.9 Hz); 7.93 (ddd, 1H, J = 8.9, 7.3, 1.6 Hz); 7.82 (d, 2H, J = 8.6 Hz); 7.40 (d, 2H, J = 8.6 Hz); 7.18 (ddd, 1H, J = 7.3, 5.1, 1.1 Hz); 5.93 (s, 1H); ¹³C NMR (CDCl₃) δ 157 (C^{IV}); 154 (C^{IV}); 151 (C^{IV}); 145 (CH); 140 (CH); 134 (C^{IV}); 131 (C^{IV}); 128 (2CH); 127 (2CH); 120 (CH); 112 (CH); 86 (CH); LC-MS (ESI) m/z 272 (MH⁺), t_r 3.45 min, λ_{max} 289 nm; HRMS (ESI-TOF) m/z [M-H]⁻ calcd for C₁₄H₉ClN₃O 270.0429, found 270.0437.

1-(Pyridin-2-yl)-3-(p-tolyl)-1H-pyrazol-5-ol (14). The solvent was removed under reduced pressure and the formed solid was recrystallized with ethanol. A brown powder was obtained: yield 33% (293 mg); mp 97 \pm 1 °C; ¹H NMR (CDCl₃) δ 12.79 (br, 1H); 8.29 (ddd, 1H, J = 5.1, 1.5, 0.9 Hz); 8.08 (ddd, 1H, J = 8.9, 1.1, 0.9 Hz); 7.93 (ddd, 1H, J = 8.9, 7.3, 1.6 Hz); 7.78 (d, 2H, J = 8.1 Hz); 7.25 (d, 2H, J = 8.1 Hz); 7.18 (ddd, 1H, J = 7.3, 5.1, 1.1 Hz); 5.94 (s, 1H); 2.41 (s, 3H); ¹³C NMR (CDCl₃) δ 157 (C^{IV}); 154 (C^{IV}); 152 (C^{IV}); 145 (CH); 140 (CH); 138 (C^{IV}); 130 (C^{IV}); 129 (2CH); 127 (2CH); 120 (CH); 112 (CH); 86 (CH); 21(CH₃); LC-MS (ESI) m/z 252 (MH⁺), t_r 3.24 min, λ_{max} 261 nm; HRMS (ESI-TOF) m/z [M+H]⁺ calcd for C₁₅H₁₄N₃O 252.1131, found 252.1131.

3-(4-Nitrophenyl)-1-(pyridin-2-yl)-1H-pyrazol-5-ol (15). The formed precipitate was filtered and washed with ethanol. A yellow powder was obtained: yield 95% (560 mg); mp $204 \pm 1^\circ\text{C}$; δ ^1H NMR (CDCl_3) δ 12.79 (br, 1H); 8.35 (ddd, 1H, $J = 5.1, 1.5, 0.9$ Hz); 8.29 (m, 2H); 8.08 (ddd, 1H, $J = 8.9, 1.1, 0.9$ Hz); 8.04 (m, 2H); 7.98 (ddd, 1H, $J = 8.9, 7.3, 1.6$ Hz); 7.25 (ddd, 1H, $J = 7.3, 5.1, 1.1$ Hz); 6.04 (s, 1H); ^{13}C NMR (CDCl_3) δ 157 (C^{IV}); 154 (C^{IV}); 150 (C^{IV}); 147 (C^{IV}); 145 (CH); 140 (CH); 139 (C^{IV}); 126 (2CH); 123 (2CH); 120 (CH); 112 (CH); 86 (CH); LC-MS (ESI) m/z 283 (MH^+), t_r 3.18 min, λ_{max} 327 nm; HRMS (ESI-TOF) m/z $[\text{M-H}]^-$ calcd for $\text{C}_{14}\text{H}_9\text{N}_4\text{O}_3$ 281.0674, found 281.0674.

3-(4-Fluorophenyl)-1-(pyridin-2-yl)-1H-pyrazol-5-ol (16). The formed precipitate was filtered and washed with ethanol (Fraction 1: 310 mg). The filtrate was concentrated under reduced pressure, diluted with ethyl acetate and purified by flash chromatography (cyclohexane/AcOEt 1:0 \rightarrow 5:5) (Fraction 2: 200 mg). Two fractions of light grey powder were obtained: yield 84% (510 mg); mp $163 \pm 1^\circ\text{C}$; ^1H NMR (CDCl_3) δ 12.81 (br, 1H); 8.29 (ddd, 1H, $J = 5.1, 1.5, 0.9$ Hz); 8.05 (ddd, 1H, $J = 8.9, 1.1, 0.9$ Hz); 7.93 (ddd, 1H, $J = 8.9, 7.3, 1.6$ Hz); 7.86 (m, 2H); 7.20 (ddd, 1H, $J = 7.3, 5.1, 1.1$ Hz); 7.12 (m, 2H); 5.92 (s, 1H); ^{13}C NMR (CDCl_3) δ 164-161 (d, $J_{\text{CF}} = 247$ Hz, C^{IV}); 157 (C^{IV}); 154 (C^{IV}); 152 (C^{IV}); 145 (CH); 140 (CH); 129 (d, $J_{\text{CF}} = 3$ Hz, C^{IV}); 127 (d, $J_{\text{CF}} = 8$ Hz, 2CH); 120 (CH); 115 (d, $J_{\text{CF}} = 21$ Hz, 2CH); 112 (CH); 86 (CH); LC-MS (ESI) m/z 256 (MH^+), t_r 3.15 min, λ_{max} 293 nm; HRMS (ESI-TOF) m/z $[\text{M+H}]^+$ calcd for $\text{C}_{14}\text{H}_{11}\text{FN}_3\text{O}$ 256.0881, found 256.0879.

3-(3,4-Dimethoxyphenyl)-1-(pyridine-2-yl)-1H-pyrazol-5-ol (17). The solvent was removed under reduced pressure. The solid obtained was purified by flash chromatography (cyclohexane/AcOEt 1:0 \rightarrow 5:5). A light yellow powder was obtained: yield 76% (180 mg); mp $165 \pm 1^\circ\text{C}$; ^1H NMR (CDCl_3) δ 12.85 (br, 1H); 8.29 (ddd, 1H, $J = 5.1, 1.5, 0.9$ Hz); 8.05 (ddd, 1H, $J = 8.9, 1.1, 0.9$ Hz); 7.93 (ddd, 1H, $J = 8.9, 7.3, 1.6$ Hz); 7.49 (d, 1H, $J = 1.8$ Hz); 7.37 (dd, 1H, $J = 8.3, 1.8$ Hz); 7.18 (ddd, 1H, $J = 7.3, 5.1, 1.1$ Hz); 6.93 (d, 1H, $J = 8.3$ Hz); 5.99 (s, 1H); 3.94 (s, 3H); ^{13}C NMR (CDCl_3) δ 157 (C^{IV}); 154 (C^{IV}); 152 (C^{IV}); 149.6 (C^{IV}); 149.0 (C^{IV}); 145 (CH); 140 (CH); 126 (C^{IV}); 119 (CH); 118 (CH); 112 (CH); 111 (C^{IV}); 85 (CH); 56 (2CH₃); LC-MS (ESI) m/z 298 (MH^+), t_r 2.67 min, λ_{max} 302 nm; HRMS (ESI-TOF) m/z $[\text{M+H}]^+$ calcd for $\text{C}_{16}\text{H}_{16}\text{N}_3\text{O}_3$ 298.1186, found 298.1184.

1-(Pyridin-2-yl)-3-(3,4,5-trimethoxyphenyl)-1H-pyrazol-5-ol (18). The solvent was removed under reduced pressure. The solid obtained was purified by flash chromatography (cyclohexane/AcOEt 1:0 \rightarrow 5:5). A light yellow powder was obtained: yield 85% (490 mg);

mp $142 \pm 1^\circ\text{C}$; $^1\text{H NMR}$ (CDCl_3) δ 12.83 (br, 1H); 8.29 (ddd, 1H, $J = 5.1, 1.5, 0.9$ Hz); 8.07 (ddd, 1H, $J = 8.9, 1.1, 0.9$ Hz); 7.91 (ddd, 1H, $J = 8.9, 7.3, 1.6$ Hz); 7.18 (ddd, 1H, $J = 7.3, 5.1, 1.1$ Hz); 7.10 (s, 2H); 5.99 (s, 1H); 3.96 (s, 6H); 3.90 (s, 3H); $^{13}\text{C NMR}$ (CDCl_3) δ 157 (C^{IV}); 155 (C^{IV}); 154 (C^{IV}); 152 (C^{IV}); 145 (CH); 140 (CH); 139 (C^{IV}); 129 (C^{IV}); 120 (CH); 112 (CH); 103 (2CH); 86 (CH); 61 (CH_3); 56 (2 CH_3); LC-MS (ESI) m/z 328 (MH^+), t_r 2.79 min, λ_{max} 298 nm; HRMS (ESI-TOF) m/z $[\text{M}+\text{H}]^+$ calcd for $\text{C}_{17}\text{H}_{18}\text{N}_3\text{O}_4$ 328.1292, found 328.1289.

3-(2,4-Dichlorophenyl)-1-(pyridin-2-yl)-1H-pyrazol-5-ol (19). The solvent was removed under reduced pressure. The solid obtained was purified by flash chromatography (cyclohexane/AcOEt 1:0 \rightarrow 5:5). An off-white powder was obtained: yield 95% (500 mg); mp $137 \pm 1^\circ\text{C}$; $^1\text{H NMR}$ (CDCl_3) δ 12.88 (br, 1H); 8.34 (ddd, 1H, $J = 5.1, 1.5, 0.9$ Hz); 8.10 (ddd, 1H, $J = 8.9, 1.1, 0.9$ Hz); 7.96 (ddd, 1H, $J = 8.9, 7.3, 1.6$ Hz); 7.86 (d, 1H, $J = 8.4$ Hz); 7.50 (d, 1H, $J = 1.8$ Hz); 7.35 (dd, 1H, $J = 8.4, 1.8$ Hz); 7.25 (ddd, 1H, $J = 7.3, 5.1, 1.1$ Hz); 6.16 (s, 1H); $^{13}\text{C NMR}$ (CDCl_3) δ 156 (C^{IV}); 154 (C^{IV}); 149 (C^{IV}); 145 (CH); 140 (CH); 134 (C^{IV}); 133 (C^{IV}); 131 (CH); 130 (CH); 129 (C^{IV}); 127 (CH); 120 (CH); 112 (CH); 90 (CH); LC-MS (ESI) m/z 306 (MH^+), t_r 3.68 min, λ_{max} 210 nm; HRMS (ESI-TOF) m/z $[\text{M}+\text{H}]^+$ calcd for $\text{C}_{14}\text{H}_{10}\text{Cl}_2\text{N}_3\text{O}$ 306.0195, found 306.0203.

3-(3,4-Dichlorophenyl)-1-(pyridin-2-yl)-1H-pyrazol-5-ol (20). The solvent was removed under reduced pressure and the formed solid was recrystallized with ethanol. A brown powder was obtained: yield 47% (202 mg); mp $175 \pm 1^\circ\text{C}$; $^1\text{H NMR}$ (CDCl_3) δ 12.79 (br, 1H); 8.33 (ddd, 1H, $J = 5.1, 1.5, 0.9$ Hz); 8.07 (ddd, 1H, $J = 8.9, 1.1, 0.9$ Hz); 8.00 (d, 1H, $J = 2.0$ Hz); 7.96 (ddd, 1H, $J = 8.9, 7.3, 1.6$ Hz); 7.68 (dd, 1H, $J = 8.4, 2.0$ Hz); 7.50 (d, 1H, $J = 8.4$ Hz); 7.20 (ddd, 1H, $J = 7.3, 5.1, 1.1$ Hz); 5.93 (s, 1H); $^{13}\text{C NMR}$ (CDCl_3) δ 157 (C^{IV}); 154 (C^{IV}); 150 (C^{IV}); 145 (CH); 140 (CH); 133.0 (C^{IV}); 132.7 (C^{IV}); 132.2 (C^{IV}); 130 (CH); 127 (CH); 125 (CH); 120 (CH); 112 (CH); 86 (CH); LC-MS (ESI) m/z 306 (MH^+), t_r 3.72 min, λ_{max} 289 nm; HRMS (ESI-TOF) m/z $[\text{M}+\text{H}]^+$ calcd for $\text{C}_{14}\text{H}_{10}\text{Cl}_2\text{N}_3\text{O}$ 304.0048, found 304.0047.

3-(4-Chloro-2-methoxyphenyl)-1-(pyridin-2-yl)-1H-pyrazol-5-ol (21). The solvent was removed under reduced pressure. The solid obtained was purified by flash chromatography (cyclohexane/AcOEt 1:0 \rightarrow 5:5). A light yellow powder was obtained: yield 95% (440 mg); mp $145 \pm 1^\circ\text{C}$; $^1\text{H NMR}$ (CDCl_3) δ 12.79 (br, 1H); 8.29 (ddd, 1H, $J = 5.1, 1.5, 0.9$ Hz); 8.10 (ddd, 1H, $J = 8.9, 1.1, 0.9$ Hz); 7.98 (d, 1H, $J = 8.2$ Hz); 7.91 (ddd, 1H, $J = 8.9, 7.3, 1.6$ Hz);

7.18 (ddd, 1H, $J = 7.3, 5.1, 1.1$ Hz); 7.04 (dd, 1H, $J = 8.2, 2.0$ Hz); 6.99 (d, 1H, $J = 2.0$ Hz); 5.99 (s, 1H); 3.94 (s, 3H); ^{13}C NMR (CDCl_3) δ 157 (C^{IV}); 154 (C^{IV}); 152 (C^{IV}); 145 (CH); 139 (CH); 119 (CH); 112 (CH); 86 (CH); LC-MS (ESI) m/z 302 (MH^+), t_r 3.30 min, λ_{max} 210 nm; HRMS (ESI-TOF) m/z $[\text{M}+\text{H}]^+$ calcd for $\text{C}_{15}\text{H}_{13}\text{ClN}_3\text{O}_2$ 302.0691, found 302.0689.

3-((3r,5r,7r)-adamantan-1-yl)-1-(pyridin-2-yl)-1H-pyrazol-5-ol (28). The formed precipitate was filtered and washed with ethanol. A brown powder was obtained: yield 95% (460 mg); mp $170 \pm 1^\circ\text{C}$; δ ^1H NMR (CDCl_3) δ 8.25 (ddd, 1H, $J = 5.1, 1.5, 0.9$ Hz); 8.17 (ddd, 1H, $J = 8.9, 1.1, 0.9$ Hz); 7.90 (ddd, 1H, $J = 8.9, 7.3, 1.6$ Hz); 7.15 (ddd, 1H, $J = 7.3, 5.1$ Hz, 1.1 Hz); 5.13 (s, 1H); 2.09 (m, 3H); 2.00 (m, 6H); 1.79 (m, 6H); ^{13}C NMR (CDCl_3) δ 157 (C^{IV}); 154 (C^{IV}); 144 (CH); 138 (C^{IV}); 140 (CH); 120 (CH); 112 (CH); 86 (CH); 40 (3CH_2); 37 (C^{IV}); 37 (3CH_2); 28 (3CH); LC-MS (ESI) m/z 296 (MH^+), t_r 3.73 min, λ_{max} 250 nm; HRMS (ESI-TOF) m/z $[\text{M}+\text{H}]^+$ calcd for $\text{C}_{18}\text{H}_{22}\text{N}_3\text{O}$ 296.1757, found 296.1753.

1,3-di(Pyridin-2-yl)-1H-pyrazol-5-ol (29). The solvent was removed under reduced pressure. The solid obtained was recrystallized in ethanol and filtered (Fraction 1: 450 mg). The filtrate was concentrated under reduced pressure and purified by flash chromatography (Cyclohexane/AcOEt 1:0 \rightarrow 5:5) (Fraction 2: 260 mg). Two fractions of light yellow powder were obtained: yield 95% (710 mg); mp $149 \pm 1^\circ\text{C}$; δ ^1H NMR (CDCl_3) 12.80 (br, 1 H); 8.69 (ddd, 1H, $J = 5.1, 1.5, 0.9$ Hz); 8.31 (ddd, 1H, $J = 5.1, 1.5, 0.9$ Hz); 8.11 (ddd, 1H, $J = 8.9, 1.1, 0.9$ Hz); 8.07 (ddd, 1H, $J = 8.9, 1.1, 0.9$ Hz); 7.92 (ddd, 1H, $J = 8.9, 7.3, 1.6$ Hz); 7.76 (ddd, 1H, $J = 8.9, 7.3, 1.6$ Hz); 7.25 (ddd, 1H, $J = 7.3, 5.1, 1.1$ Hz); 7.21 (ddd, 1H, $J = 7.3, 5.1, 1.1$ Hz); 6.27 (s, 1H); ^{13}C NMR (CDCl_3); LC-MS (ESI) m/z 239 (MH^+), ^{13}C NMR (CDCl_3) δ 157 (C^{IV}); 154 (C^{IV}); 153 (C^{IV}); 152 (C^{IV}); 149 (CH); 145 (CH); 140 (CH); 136 (CH); 123 (CH); 120 (2CH); 112 (CH); 86 (CH); LC-MS (ESI) 239 m/z t_r 2.38 min, λ_{max} 295 nm; HRMS (ESI-TOF) m/z $[\text{M}+\text{H}]^+$ calcd for $\text{C}_{13}\text{H}_{11}\text{N}_4\text{O}$ 239.0927, found 239.0925.

3-((3r,5r,7r)-adamantan-1-yl)-1-(pyridin-3-yl)-1H-pyrazol-5(4H)-one (30). The formed precipitate was filtered and washed with ethanol. A light brown powder was obtained: yield 95% (465 mg); mp $178 \pm 1^\circ\text{C}$; δ ^1H NMR (CDCl_3) 9.21 (d, 1H, $J = 0.9$ Hz); 8.45 (ddd, 1H, $J = 4.6, 2.1, 0.9$ Hz); 8.37 (ddd, 1H, $J = 8.4, 2.1, 1.4$ Hz); 7.40 (dd, 1H, $J = 8.4, 4.6$ Hz); 3.46 (s, 2H); 2.13 (m, 3H); 1.91 (m, 6H); 1.78 (m, 6H); ^{13}C NMR (CDCl_3) δ 171 (C^{IV}); 168 (C^{IV}); 144 (CH); 140 (CH); 135 (C^{IV}); 126 (CH); 123 (CH); 86 (CH); 40 (3CH_2); 37 (CH^2); 37

(C^{IV}); 36 (3CH₂) 28 (3CH); (LC-MS (ESI) *m/z* 296 (MH⁺), *t_r* 2.98 min, λ_{max} 243 nm; HRMS (ESI-TOF) *m/z* [M+H]⁺ calcd for C₁₈H₂₂N₃O 296.1757, found 296.1755.

3-((3r,5r,7r)-adamantan-1-yl)-1-(pyridin-4-yl)-1H-pyrazol-5(4H)-one (31). The formed precipitate was filtered and washed with ethanol. A light brown powder was obtained: yield 95% (465 mg); mp 228 ± 1°C; δ ¹H NMR (CDCl₃) 9.21 (d, 1H, *J* = 0.9 Hz); 8.45 (ddd, 1H, *J* = 4.6, 2.1, 0.9 Hz); 8.37 (ddd, 1H, *J* = 8.4, 2.1, 1.4 Hz); 7.40 (dd, 1H, *J* = 8.4, 4.6 Hz); 3.46 (s, 2H); 2.13 (m, 3H); 1.91 (m, 6H); 1.78 (m, 6H); ¹³C NMR (CDCl₃) δ 171 (C^{IV}); 168 (C^{IV}); 144 (CH); 140 (CH); 135 (C^{IV}); 126 (CH); 123 (CH); 86 (CH); 40 (3CH₂); 38 (CH₂); 37 (C^{IV}); 36 (3CH₂) 28 (3CH); (LC-MS (ESI) *m/z* 296 (MH⁺), *t_r* 2.92 min, λ_{max} 257 nm; HRMS (ESI-TOF) *m/z* [M+H]⁺ calcd for C₁₈H₂₂N₃O 296.1757, found 296.1752.

3-((3r,5r,7r)-adamantan-1-yl)-1-(2,4-dichlorophenyl)-1H-pyrazol-5-ol (32). The formed precipitate was filtered and washed with ethanol. A white powder was obtained: yield 86% (256 mg); mp 218 ± 1°C; ¹H NMR (DMSO) δ 11.11 (br, 1H); 7.79 (d, 1H, *J* = 2.0 Hz); 7.51 (dd, 1H, *J* = 8.0, 2.0 Hz); 7.45 (d, 1H, *J* = 8.0 Hz); 5.35 (s, 1H); 1.99 (m, 3H); 1.85 (m, 6H); 1.71 (m, 6H); ¹³C NMR (DMSO) δ 162 (C^{IV}); 154 (C^{IV}); 136 (C^{IV}); 134 (C^{IV}); 132 (C^{IV}); 131 (CH); 130 (CH); 128 (CH); 82 (CH); 42 (3CH₂); 37 (3CH₂); 34 (C^{IV}); 28 (3CH) ; LC-MS (ESI) *m/z* 363 (MH⁺), *t_r* 3.52 min, λ_{max} 210 nm; HRMS (ESI-TOF) *m/z* [M+H]⁺ calcd for C₁₉H₂₁Cl₂N₂O 363.1026, found 363.1017.

3-((3r,5r,7r)-adamantan-1-yl)-1-(2,4-dimethylphenyl)-1H-pyrazol-5(4H)-one (33). The formed precipitate was filtered and washed with ethanol. A light brown solid was obtained: yield 88% (275 mg); mp 230 ± 1°C; ¹H NMR (CDCl₃) δ 7.22 (d, 1H, *J* = 8.0 Hz); 7.08 (m, 2H); 3.38 (s, 2H); 2.09 (m, 3H); 1.88 (m, 6H); 1.76 (m, 6H); ¹³C NMR (CDCl₃) δ 171 (C^{IV}); 167 (C^{IV}); 138 (C^{IV}); 135 (C^{IV}); 133 (C^{IV}); 132 (CH); 127 (CH); 126 (CH); 40 (3CH₂); 36.9 (C^{IV}); 36.7 (CH₂); 36.5 (3CH₂); 28 (3CH); 21 (CH₃); 18 (CH₃); LC-MS (ESI) *m/z* 323 (MH⁺), *t_r* 3.35 min, λ_{max} 210 nm; HRMS (ESI-TOF) *m/z* [M+H]⁺ calcd for C₂₁H₂₇N₂O 323.2118, found 323.2116.

3-((3r,5r,7r)-adamantan-1-yl)-1-(2,4-diaminophenyl)-1H-pyrazol-5(4H)-one (34). The formed precipitate was filtered and washed with ethanol. A light brown solid was obtained: yield 90% (280 mg); 155 ± 1°C; ¹H NMR (CDCl₃) δ 8.62 (d, 2H, *J* = 6.5 Hz); 8.22 (d, 2H, *J* = 6.5 Hz); 3.56 (s, 2H); 2.13 (m, 3H); 1.88 (m, 6H); 1.76 (m, 6H); ¹³C NMR (CDCl₃) δ 171 (C^{IV}); 169 (C^{IV}); 148 (C^{IV}); 145 (2CH); 112 (2CH); 40 (3CH₂); 38 (CH₂); 37 (C^{IV}); 36

(3CH₃); 28 (3CH); LC-MS (ESI) *m/z* 325 (MH⁺), *t_r* 2.35 min, λ_{max} 220 nm; HRMS (ESI-TOF) *m/z* [M+H]⁺ calcd for C₁₉H₂₅N₄O 325.2023, found 325.2025.

3-((3r,5r,7r)-adamantan-1-yl)-1-phenyl-1H-pyrazol-5(4H)-one (35) The formed precipitate was filtered and washed with ethanol. A white solid was obtained: yield 85% (287 mg); mp 138 ± 1°C; ¹H NMR (CDCl₃) δ 7.93 (m, 2H); 7.42 (m, 2H); 7.21 (m, 1H); 3.43 (s, 2H); 2.09 (m, 3H); 1.88 (m, 6H); 1.76 (m, 6H); ¹³C NMR (CDCl₃) δ 170 (C^{IV}); 166 (C^{IV}); 138 (C^{IV}); 129 (2CH); 125 (CH); 119 (2CH); 40 (3CH₂); 38 (CH₂); 37 (C^{IV}); 36 (3CH₂); 28 (3CH); LC-MS (ESI) *m/z* 295 (MH⁺), *t_r* 3.56 min, λ_{max} 243 nm; HRMS (ESI-TOF) *m/z* [M+H]⁺ calcd for C₁₉H₂₃N₂O 295.1805, found 295.1789.

3-(2-Methoxyphenyl)-1-(pyrimidin-2-yl)-1H-pyrazol-5-ol (36). The solvent was removed under reduced pressure. The solid obtained was purified by flash chromatography (cyclohexane/AcOEt 1:0 → 8:2). A purple powder was obtained: yield 83% (200 mg); mp 153 ± 1°C; ¹H NMR (CDCl₃) δ 11.79 (br, 1H); 8.76 (d, 2H, *J* = 4.9 Hz); 8.15 (m, 1H); 7.36 (ddd, 1H, *J* = 8.5, 7.6, 1.9 Hz); 7.21 (t, 1H, *J* = 4.9 Hz); 7.04 (m, 1H); 6.98 (dd, 1H, *J* = 8.5, 0.9 Hz); 6.27 (s, 1H); 3.91 (s, 3H); ¹³C NMR (CDCl₃) δ 158.2 (2CH); 157.4 (2C^{IV}); 156 (C^{IV}); 152 (C^{IV}); 130 (CH); 129.4 (CH); 121.5 (C^{IV}); 120.6 (CH); 117 (CH); 111 (CH); 91 (CH); 55 (CH₃); LC-MS (ESI) *m/z* 269 (MH⁺), *t_r* 2.22 min, λ_{max} 273 nm; HRMS (ESI-TOF) *m/z* [M+H]⁺ calcd for C₁₄H₁₃N₄O₂ 269.1033, found 269.1031.

1-(3-Fluoropyridin-2-yl)-3-(2-methoxyphenyl)-1H-pyrazol-5(4H)-one (37). The solvent was removed under reduced pressure. The solid obtained was purified by flash chromatography (cyclohexane/AcOEt 1:0 → 8:2). A light yellow powder was obtained: yield 85% (250 mg); mp 179 ± 1°C; ¹H NMR (CDCl₃) δ 8.44 (ddd, 1H, *J* = 4.7, 1.5, 1.0 Hz); 8.05 (dd, 1H, *J* = 7.6, 1.8 Hz); 7.63 (ddd, 1H, *J* = 10.4, 8.1, 1.5 Hz); 7.42 (ddd, 1H, *J* = 9.0, 7.6, 1.8 Hz); 7.36 (ddd, 1H, *J* = 8.1, 4.7, 3.0 Hz); 6.99 (td, 1H, *J* = 7.6, 1.0 Hz); 6.98 (dd, 1H, *J* = 9.0, 1.0 Hz); 4.08 (s, 2H); 3.94 (s, 3H); ¹³C NMR (CDCl₃) δ 172 (C^{IV}); 158 (C^{IV}); 155 (C_i); 154-151 (d, *J_{CF}* = 264 Hz, C^{IV}); 145 (d, *J_{CF}* = 5.5 Hz, CH); 138 (d, *J_{CF}* = 12.6 Hz, C^{IV}); 132 (CH); 128 (CH); 125 (d, *J_{CF}* = 18 Hz, CH); 124 (d, *J_{CF}* = 4 Hz, CH), CH; 121 (CH); 120 (C^{IV}); 111 (CH); 55 (CH₃); 42 (CH₂); LC-MS (ESI) *m/z* 286 (MH⁺), *t_r* 2.22 min, λ_{max} 215 nm; HRMS (ESI-TOF) *m/z* [M+H]⁺ calcd for C₁₅H₁₃FN₃O₂ 286.0986, found 286.0983.

1-(3,5-Difluoropyridin-2-yl)-3-(2-methoxyphenyl)-1H-pyrazol-5(4H)-one (38). The solvent was removed under reduced pressure. The solid obtained was purified by flash

chromatography (cyclohexane/AcOEt 1:0 → 5:5). A light yellow powder was obtained: yield 73% (200 mg); mp $174 \pm 1^\circ\text{C}$; ^1H - $\{^{19}\text{F}\}$ NMR (CDCl_3) δ 8.36 (dd, 1H, $J = 2.5, 0.6$ Hz); 8.02 (dd, 1H, $J = 7.6, 1.8$ Hz); 7.42 (m, 2H); 7.03 (td, 1H, $J = 7.6, 1.0$ Hz); 6.99 (dd, 1H, $J = 9.0, 1.0$ Hz); 4.06 (1H, s); 3.91 (s, 3H); ^{13}C NMR (CDCl_3) δ 171 (C^{IV}); 157 (C^{IV}); 156 (dd, $J_{\text{CF}} = 450$ Hz, 5 Hz, C^{IV}); 155 (C^{IV}); 153 (dd, $J_{\text{CF}} = 450$ Hz, 5 Hz, C^{IV}); 135 (dd, $J_{\text{CF}} = 24$ Hz, 5 Hz, CH); 133 (CH); 128 (CH); 121 (CH); 119 (C^{IV}); 113 (dd, $J_{\text{CF}} = 22$ Hz, 21 Hz, CH); 111 (CH); 55 (CH_3); 44 (CH_2); LC-MS (ESI) m/z 304 (MH^+), t_r 2.33 min, λ_{max} 210 nm; HRMS (ESI-TOF) m/z $[\text{M}+\text{H}]^+$ calcd for $\text{C}_{15}\text{H}_{12}\text{F}_2\text{N}_3\text{O}_2$ 304.0892, found 304.0888.

1-(4-Chloropyridin-2-yl)-3-(2-methoxyphenyl)-1H-pyrazol-5(4H)-one (39). The formed precipitate was filtered and washed with ethanol (Fraction 1: 150 mg). The filtrate was concentrated under reduced pressure, recrystallized in ethanol (Fraction 2: 110 mg). Two fractions of light yellow powder were obtained: yield 95% (260 mg); mp $209 \pm 1^\circ\text{C}$; ^1H NMR (CDCl_3) δ 8.35 (d, 1H, $J = 5.7$ Hz); 8.06 (dd, 1H, $J = 7.8, 1.7$ Hz); 8.02 (d, 1H, $J = 1.7$ Hz); 7.98 (dd, 1H, $J = 5.7, 1.7$ Hz); 7.46 (dd, 1H, $J = 8.5, 7.5, 1.7$ Hz); 7.05 (td, 1H, $J = 7.5, 0.9$ Hz); 6.98 (dd, 1H, $J = 8.5, 0.9$ Hz); ^{13}C NMR (CDCl_3) δ 172 (C^{IV}); 158 (C^{IV}); 155 (C^{IV}); 152 (C^{IV}); 150 (CH); 146 (C^{IV}); 132 (CH); 128 (CH); 121 (CH); 119 (C^{IV}); 111.9 (CH); 111.6 (C); 110 (CH); 55 (CH_3); 44 (CH_2); LC-MS (ESI) m/z 302 (MH^+), t_r 2.87 min, λ_{max} 210 nm; HRMS (ESI-TOF) m/z $[\text{M}-\text{H}]^-$ calcd for $\text{C}_{15}\text{H}_{11}\text{ClN}_3\text{O}_2$ 300.0534, found 304.0539.

1-(3,5-Dichloropyridin-2-yl)-3-(2-methoxyphenyl)-1H-pyrazol-5(4H)-one (40). The solvent was removed under reduced pressure. The solid obtained was purified by flash chromatography (cyclohexane/AcOEt 1:0 → 5:5). A light yellow powder was obtained: yield 95% (320 mg); mp $133 \pm 1^\circ\text{C}$; ^1H NMR (CDCl_3) δ 8.50 (d, 1H, $J = 2.3$ Hz); 8.00 (dd, 1H, $J = 7.8, 1.7$ Hz); 7.93 (d, 1H, $J = 2.3$ Hz); 7.44 (ddd, 1H, $J = 8.5, 7.5, 1.7$ Hz); 6.99 (m, 2H); 4.06 (s, 2H); 3.92 (s, 3H); ^{13}C NMR (CDCl_3) δ 171 (C^{IV}); 158 (C^{IV}); 155 (C^{IV}); 146 (CH); 145 (C^{IV}); 139 (CH); 132 (CH); 131 (C^{IV}); 129 (C^{IV}); 128 (CH); 121 (CH); 120 (C^{IV}); 111 (CH); 55 (CH_3); 42 (CH_2); LC-MS (ESI) m/z 336 (MH^+), t_r 2.60 min, λ_{max} 210 nm; HRMS (ESI-TOF) m/z $[\text{M}+\text{H}]^+$ calcd for $\text{C}_{15}\text{H}_{12}\text{Cl}_2\text{N}_3\text{O}_2$ 336.0301, found 336.0289.

General procedure for preparation of alkylated pyrazolones (22-27)

The corresponding β -keto ester (1 eq.) and hydrazine (1.5 eq.) were dissolved in glacial acetic acid (6M). The mixture was subjected to microwave irradiations for 2.5-5 minutes at 130°C and 150W. The reaction was followed by TLC. The acetic acid was then evaporated under reduced pressure.

3-Methyl-1-(pyridin-2-yl)-1H-pyrazol-5-ol (22). The solvent was removed under reduced pressure. The solid obtained was purified by flash chromatography (cyclohexane/AcOEt 1:0 → 8:2). A light yellow powder was obtained: yield 95% (450 mg); mp $110 \pm 1^\circ\text{C}$ ^1H NMR (CDCl_3) δ 12.57 (br, 1H); 7.87 (ddd, 1H, $J = 5.1, 1.6, 0.9$ Hz); 7.85 (ddd, 1H, $J = 8.9, 1.1, 0.9$ Hz); 7.83 (ddd, 1H, $J = 8.9, 7.3, 1.6$ Hz); 7.10 (ddd, 1H, $J = 7.3, 5.1, 1.1$ Hz); 5.42 (s, 1H); 2.55 (s, 3H); ^{13}C NMR (CDCl_3) δ 157 (C^{IV}); 154 (C^{IV}); 151 (C^{IV}); 145 (CH); 139 (CH); 119 (CH); 112 (CH); 89 (CH); 14 (CH_3); LC-MS (ESI) m/z 176 (MH^+), t_r 1.72 min, λ_{max} 243 nm; HRMS (ESI-TOF) m/z $[\text{M}+\text{H}]^+$ calcd for $\text{C}_9\text{H}_{10}\text{N}_3\text{O}$ 176.0818, found 176.0814.

3-Ethyl-1-(pyridin-2-yl)-1H-pyrazol-5-ol (23). The solvent was removed under reduced pressure. The solid obtained was purified by flash chromatography (cyclohexane/AcOEt 1:0 → 8:2). A light yellow powder was obtained: yield 95% (600 mg); mp $88 \pm 1^\circ\text{C}$; ^1H NMR (CDCl_3) δ 12.66 (br, 1H); 8.18 (ddd, 1H, $J = 5.1, 1.6, 0.9$ Hz); 7.80 (m, 2H); 7.08 (m, 1H); 5.43 (s, 1H); 2.58 (q, 2H, $J = 7.6$ Hz); 1.25 (t, 3H, $J = 7.6$ Hz); ^{13}C NMR (CDCl_3) δ 157 (C^{IV}); 154 (C^{IV}); 148 (C^{IV}); 145 (CH); 139 (CH); 119 (CH); 112 (CH); 87 (CH); 22 (CH_2); 13 (CH_3); LC-MS (ESI) m/z 190 (MH^+), t_r 1.98 min, λ_{max} 275 nm; HRMS (ESI-TOF) m/z $[\text{M}+\text{H}]^+$ calcd for $\text{C}_{10}\text{H}_{12}\text{N}_3\text{O}$ 190.0975, found 190.0971.

3-Propyl-1-(pyridin-2-yl)-1H-pyrazol-5-ol (24). The solvent was removed under reduced pressure. The solid obtained was purified by flash chromatography (cyclohexane/AcOEt 1:0 → 8:2). A light yellow powder was obtained: yield 95% (660 mg); mp $84 \pm 1^\circ\text{C}$; ^1H NMR (CDCl_3) δ 12.74 (br, 1H); 8.24 (ddd, 1H, $J = 5.1, 1.6, 0.9$ Hz); 7.85 (m, 2H); 7.08 (m, 1H); 5.44 (s, 1H); 2.55 (t, 2H, $J = 8.0$ Hz); 1.65 (sext, 2H, $J = 8.0$ Hz); 1.00 (t, 3H, $J = 8.0$ Hz); ^{13}C NMR (CDCl_3) δ 157 (C^{IV}); 154 (C^{IV}); 150 (C^{IV}); 145 (CH); 139 (CH); 119 (CH); 112 (CH); 87 (CH); 31 (CH_2); 22 (CH_2); 14 (CH_3); LC-MS (ESI) m/z 204 (MH^+), t_r 2.36 min, λ_{max} 248 nm; HRMS (ESI-TOF) m/z $[\text{M}+\text{H}]^+$ calcd for $\text{C}_{11}\text{H}_{14}\text{N}_3\text{O}$ 204.1131, found 204.1134.

3-Butyl-1-(pyridin-2-yl)-1H-pyrazol-5-ol (25). The solvent was removed under reduced pressure. The solid obtained was purified by flash chromatography (cyclohexane/AcOEt 1:0 → 8:2). A light yellow powder was obtained: yield 95% (260 mg); mp $69 \pm 1^\circ\text{C}$; ^1H NMR (CDCl_3) δ 12.70 (s, 1H); 8.25 (ddd, 1H, $J = 5.1, 1.6, 0.9$ Hz); 8.00 (ddd, 1H, $J = 8.9, 1.1, 0.9$ Hz); 7.86 (ddd, 1H, $J = 8.9, 7.3, 1.6$ Hz); 7.12 (ddd, 1H, $J = 7.3, 5.1, 1.1$ Hz); 5.47 (s, 1H); 2.93 (hept, 1H, $J = 7.0$ Hz); 1.30 (d, 1H, $J = 7.0$ Hz); ^{13}C NMR (CDCl_3) 157 (C^{IV}); 154 (C^{IV}); 150 (C^{IV}); 145 (CH); 139 (CH); 119 (CH); 112 (CH); 87 (CH); 31 (CH_2); 29 (CH_2); 23 (CH_2);

14 (CH₃); LC-MS (ESI) m/z 218 (MH⁺), t_r 2.67 min, λ_{max} 272 nm; HRMS (ESI-TOF) m/z [M+H]⁺ calcd for C₁₂H₁₆N₃O 218.1288, found 218.1288.

3-Isopropyl-1-(pyridin-2-yl)-1H-pyrazol-5-ol (26). The solvent was removed under reduced pressure. The solid obtained was purified by flash chromatography (cyclohexane/AcOEt 1:0 → 8:2). A light yellow powder was obtained: yield 95% (660 mg); mp 33 ± 1°C; ¹H NMR (CDCl₃) δ 12.79 (br, 1H); 8.29 (ddd, 1H, J = 5.1, 1.5, 0.9 Hz); 8.05 (ddd, 1H, J = 8.9, 1.1, 0.9 Hz); 7.93 (ddd, 1H, J = 8.9, 7.3, 1.6 Hz); 7.18 (ddd, 1H, J = 7.3, 5.1, 1.1 Hz); 5.47 (s, 1H); 2.97 (hept, 1H, J = 6.9 Hz); 1.29 (d, 6H, J = 6.9 Hz); ¹³C NMR (CDCl₃) δ 161 (C^{IV}); 156 (C^{IV}); 154 (C^{IV}); 145 (CH); 140 (CH); 119 (CH); 112 (CH); 86 (CH); 29 (CH); 22 (2CH₃); LC-MS (ESI) m/z 204 (MH⁺), t_r 2.34 min, λ_{max} 248 nm; HRMS (ESI-TOF) m/z [M+H]⁺ calcd for C₁₁H₁₄N₃O 204.1131, found 204.1129.

3-(tert-Butyl)-1-(pyridin-2-yl)-1H-pyrazol-5-ol (27). The solvent was removed under reduced pressure. The solid obtained was purified by flash chromatography (cyclohexane/AcOEt 1:0 → 8:2). A light yellow powder was obtained: yield 91% (481 mg); mp 75 ± 1°C; ¹H NMR (CDCl₃) δ 12.60 (br, 1H); 8.22 (ddd, 1H, J = 5.1, 1.6, 0.9 Hz); 7.89 (m, 1H); 7.82 (ddd, 1H, J = 8.9, 7.3, 1.6 Hz); 7.09 (ddd, 1H, J = 7.3, 5.1, 1.1 Hz); 5.48 (s, 1H); 1.30 (s, 9H); ¹³C NMR (CDCl₃) δ 163 (C^{IV}); 157 (C^{IV}); 154 (C^{IV}); 145 (CH); 139 (CH); 119 (CH); 112 (CH); 86 (CH); 31 (C^{IV}); 30 (3CH₃); LC-MS (ESI) m/z 218 (MH⁺), t_r 2.78 min, λ_{max} 250 nm; HRMS (ESI-TOF) m/z [M+H]⁺ calcd for C₁₂H₁₆N₃O 218.1288, found 218.1289.

AUTHOR CONTRIBUTIONS

RMi, BQ and XT design the research. RLB, RM, FK, NL, GV, NR, BT, MT, HB, XD and XT performed the experiments. RLB, FK, NL, XT and RMi analyzed the data. RMi and RLB wrote the manuscript with the input of XT, BQ, NL and CB. All authors contributed to the article and approved the submitted version.

FUNDING

The project had received funding from the SIRIC OncoLille. The project was supported by a grant from the SATT Nord. This work was supported a Grant from Contrat de Plan Etat Région CPER Cancer 2015-2020.

ACKNOWLEDGMENTS

We are grateful i) to the UMS-2014 US41 PLBS for access to the cytometry Platform, ii) to U1177 for access to the ADME Platform, iii) to CUMA of University of Lille for access to NMR platform and iv) to PSM of University of Lille for HRMS experiments.

BIBLIOGRAPHY

- [1] H. Sung, J. Ferlay, R.L. Siegel, M. Laversanne, I. Soerjomataram, A. Jemal, F. Bray, Global Cancer Statistics 2020: GLOBOCAN Estimates of Incidence and Mortality Worldwide for 36 Cancers in 185 Countries, *CA. Cancer J. Clin.* 71 (2021) 209–249.
- [2] Y. Han, D. Liu, L. Li, PD-1/PD-L1 pathway: current researches in cancer, *Am. J. Cancer Res.* 10 (2020) 727–742.
- [3] G. Housman, S. Byler, S. Heerboth, K. Lapinska, M. Longacre, N. Snyder, S. Sarkar, Drug Resistance in Cancer: An Overview, *Cancers.* 6 (2014) 1769–1792.
- [4] Y. Wu, W. Chen, Z.P. Xu, W. Gu, PD-L1 Distribution and Perspective for Cancer Immunotherapy—Blockade, Knockdown, or Inhibition, *Front. Immunol.* 10 (2019). <https://doi.org/10.3389/fimmu.2019.02022>.
- [5] L. Lee, M. Gupta, S. Sahasranaman, Immune Checkpoint inhibitors: An introduction to the next-generation cancer immunotherapy, *J. Clin. Pharmacol.* 56 (2016) 157–169.
- [6] K.M. Zak, P. Grudnik, K. Magiera, A. Dömling, G. Dubin, T.A. Holak, Structural Biology of the Immune Checkpoint Receptor PD-1 and Its Ligands PD-L1/PD-L2, *Structure.* 25 (2017) 1163–1174.
- [7] Y. Dong, Q. Sun, X. Zhang, PD-1 and its ligands are important immune checkpoints in cancer, *Oncotarget.* 8 (2016) 2171–2186.
- [8] K. Li, Z. Yuan, J. Lyu, E. Ahn, S.J. Davis, R. Ahmed, C. Zhu, PD-1 suppresses TCR-CD8 cooperativity during T-cell antigen recognition, *Nat. Commun.* 12 (2021) 2746.
- [9] L. Ardolino, A. Joshua, Immune checkpoint inhibitors in malignancy, *Aust. Prescr.* 42 (2019) 62–67.
- [10] A. De Sousa Linhares, C. Battin, S. Jutz, J. Leitner, C. Hafner, J. Tobias, U. Wiedermann, M. Kundi, G.J. Zlabinger, K. Grabmeier-Pfistershammer, P. Steinberger, Therapeutic PD-L1 antibodies are more effective than PD-1 antibodies in blocking PD-1/PD-L1 signaling, *Sci. Rep.* 9 (2019) 11472.
- [11] B. Shankar, J. Naidoo, PD-1 and PD-L1 inhibitor toxicities in non-small cell lung cancer, *J. Thorac. Dis.* 10 (2018) S4034–S4037.

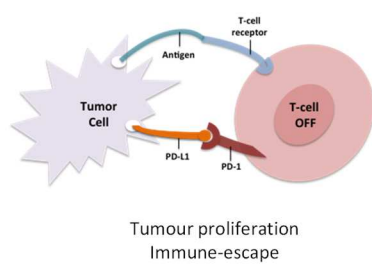
- [12] T. Ashizawa, A. Iizuka, E. Tanaka, R. Kondou, H. Miyata, C. Maeda, T. Sugino, K. Yamaguchi, T. Ando, Y. Ishikawa, M. Ito, Y. Akiyama, Antitumor activity of the PD-1/PD-L1 binding inhibitor BMS-202 in the humanized MHC-double knockout NOG mouse, *Biomed. Res. Tokyo Jpn.* 40 (2019) 243–250.
- [13] L.A. Lampson, Monoclonal antibodies in neuro-oncology: Getting past the blood-brain barrier, *MAbs.* 3 (2011) 153–160.
- [14] B. Musielak, J. Kocik, L. Skalniak, K. Magiera-Mularz, D. Sala, M. Czub, M. Stec, M. Siedlar, T.A. Holak, J. Plewka, CA-170 – A Potent Small-Molecule PD-L1 Inhibitor or Not?, *Molecules.* 24 (2019). <https://doi.org/10.3390/molecules24152804>.
- [15] T. Zarganes-Tzitzikas, M. Konstantinidou, Y. Gao, D. Krzemien, K. Zak, G. Dubin, T.A. Holak, A. Dömling, Inhibitors of programmed cell death 1 (PD-1): a patent review (2010-2015), *Expert Opin. Ther. Pat.* 26 (2016) 973–977.
- [16] L. Skalniak, K.M. Zak, K. Guzik, K. Magiera, B. Musielak, M. Pachota, B. Szelazek, J. Kocik, P. Grudnik, M. Tomala, S. Krzanik, K. Pyrc, A. Dömling, G. Dubin, T.A. Holak, Small-molecule inhibitors of PD-1/PD-L1 immune checkpoint alleviate the PD-L1-induced exhaustion of T-cells, *Oncotarget.* 8 (2017) 72167–72181.
- [17] J.-J. Park, E.P. Thi, V.H. Carpio, Y. Bi, A.G. Cole, B.D. Dorsey, K. Fan, T. Harasym, C.L. Iott, S. Kadhim, J.H. Kim, A.C.H. Lee, D. Nguyen, B.S. Paratala, R. Qiu, A. White, D. Lakshminarasimhan, C. Leo, R.K. Suto, R. Rijnbrand, S. Tang, M.J. Sofia, C.B. Moore, Checkpoint inhibition through small molecule-induced internalization of programmed death-ligand 1, *Nat. Commun.* 12 (2021) 1222.
- [18] Q. Wu, L. Jiang, S.C. Li, Q.J. He, B. Yang, J. Cao. Small molecule inhibitors targeting the PD-1/PD-L1 signaling pathway, *Acta Pharmacol. Sin.* 42 (2021) 1–9.
- [19] X. Lin, X. Lu, G. Luo, H. Xiang. Progress in PD-1/PD-L1 pathway inhibitors: From biomacromolecules to small molecules. *Eur. J. Med. Chem.* 15 (2020) 111876.
- [20] K. Li, H. Tian. Development of small-molecule immune checkpoint inhibitors of PD-1/PD-L1 as a new therapeutic strategy for tumour immunotherapy, *J. Drug Target.* 27 (2019) 244–256.
- [21] T. Wang, X. Wu, C. Guo, K. Zhang, J. Xu, Z. Li, S. Jiang. Development of Inhibitors of the Programmed Cell Death-1/Programmed Cell Death-Ligand 1 Signaling Pathway, *J. Med. Chem.* 62 (2019) 1715–1730.
- [22] J. Jiang, X. Zou, Y. Liu, X. Liu, K. Dong, X. Yao, Z. Feng, X. Chen, L. Sheng, Y. Li. Simultaneous Determination of a Novel PD-L1 Inhibitor, IMM-010, and Its Active Metabolite, YPD-29B, in Rat Biological Matrices by Polarity-Switching Liquid

- Chromatography-Tandem Mass Spectrometry: Application to ADME Studies, *Front. Pharmacol.* 21 (2021) 677120.
- [23] Y. Wang, X. Liu, X. Zou, S. Wang, L. Luo, Y. Liu, K. Dong, X. Yao, Y. Li, X. Chen, L. Sheng. Metabolism and Interspecies Variation of IMM-010, a Programmed Cell Death Ligand 1 Inhibitor Prodrug, *Pharmaceutics* 21 (2021) 598.
- [24] M. Wang, X. Ma, K. Zhou, H. Mao, J. Liu, X. Xiong, X. Zhao, S. Narva, Y. Tanaka, Y. Wu, C. Guo, H. Sugiyama, W. Zhang. Discovery of Pyrrole-imidazole Polyamides as PD-L1 Expression Inhibitors and Their Anticancer Activity via Immune and Nonimmune Pathways, *J. Med. Chem.* 64 (2021) 6021–6036.
- [25] Z. Song, B. Liu, X. Peng, W. Gu, Y. Sun, L. Xing, Y. Xu, M. Geng, J. Ai, A. Zhang. Design, Synthesis, and Pharmacological Evaluation of Biaryl-Containing PD-1/PD-L1 Interaction Inhibitors Bearing a Unique Difluoromethyleneoxy Linkage, *J. Med. Chem.* 64 (2021) 16687–16702.
- [26] T. Wang, S. Cai, M. Wang, W. Zhang, K. Zhang, D. Chen, Z. Li, S. Jiang. Novel Biphenyl Pyridines as Potent Small-Molecule Inhibitors Targeting the Programmed Cell Death-1/Programmed Cell Death-Ligand 1 Interaction, *J. Med. Chem.* 64 (2021) 7390–7403.
- [27] T. Wang, S. Cai, Y. Cheng, W. Zhang, M. Wang, H. Sun, B. Guo, Z. Li, Y. Xiao, S. Jiang. Discovery of Small-Molecule Inhibitors of the PD-1/PD-L1 Axis That Promote PD-L1 Internalization and Degradation, *J. Med. Chem.* 65 (2022) 3879–3893.
- [28] R. Magnez, B. Thiroux, S. Taront, Z. Segoula, B. Quesnel, X. Thuru, PD-1/PD-L1 binding studies using microscale thermophoresis, *Sci. Rep.* 15 (2017) 17623.
- [29] L. Knorr, Einwirkung von Acetessigester auf Phenylhydrazin, *Berichte Dtsch. Chem. Ges.* 16 (1883) 2597–2599.
- [30] A.A. Al-Mutairi, F.E.M. El-Baih, H.M. Al-Hazimi, Microwave versus ultrasound assisted synthesis of some new heterocycles based on pyrazolone moiety, *J. Saudi Chem. Soc.* 14 (2010) 287–299.
- [31] R.V. Antre, A. Cendilkumar, D. Goli, G.S. Andhale, R.J. Oswal, Microwave assisted synthesis of novel pyrazolone derivatives attached to a pyrimidine moiety and evaluation of their anti-inflammatory, analgesic and antipyretic activities, *Saudi Pharm. J.* 19 (2011) 233–243.
- [32] M.M. Mojtahedi, M. Javadpour, M.S. Abaee, Convenient ultrasound mediated synthesis of substituted pyrazolones under solvent-free conditions, *Ultrason. Sonochem.* 15 (2008) 828–832.

- [33] Y. Xu, J. Cuccui, C. Denman, T. Maharjan, B.W. Wren, G.K. Wagner, Structure-activity relationships in a new class of non-substrate-like covalent inhibitors of the bacterial glycosyltransferase LgtC, *Bioorg. Med. Chem.* 26 (2018) 2973–2983.
- [34] L. Shi, K. Li, P.-C. Cui, L.-L. Li, S.-L. Pan, M.-Y. Li, X.-Q. Yu, BINOL derivatives with aggression-induced emission, *J. Mater. Chem. B.* 6 (2018) 4413–4416.
- [35] R.J. Clay, T.A. Collom, G.L. Karrick, J. Wemple, A Safe, Economical Method for the Preparation of β -Oxo Esters, *Synthesis*. 1993 (1993) 290–292.
- [36] P. Drouhin, R.J.K. Taylor, A Copper-Mediated Oxidative Coupling Route to 3H- and 1H-Indoles from N-Aryl-enamines, *Eur. J. Org. Chem.* 2015 (2015) 2333–2336.
- [37] C. Bailly, G. Vergoten. N-glycosylation and ubiquitinylation of PD-L1 do not restrict interaction with BMS-202: A molecular modeling study. *Comput. Biol. Chem.* 88 (2020) 107362.
- [38] W.L. Jorgensen, J.P. Ulmschneider, J. Tirado-Rives. Free energies of hydration from a generalized Born model and an ALL-atom force field, *J. Phys. Chem. B* 108 (2004) 16264–16270.
- [39] A. Zafar, J. Reynisson. Hydration Free Energy as a Molecular Descriptor in Drug Design: A Feasibility Study, *Mol. Inform.* 35 (2016) 207–214.
- [40] R. Belani, G.J. Weiner. Expression of both B7-1 and CD28 contributes to the IL-2 responsiveness of CTLL-2 cells, *Immunology* 87 (1996) 271–274.
- [41] M.J. Butte, M.E. Keir, T.B. Phamduy, A.H. Sharpe, G.J. Freeman. Programmed death-1 ligand 1 interacts specifically with the B7-1 costimulatory molecule to inhibit T cell responses, *Immunity* 27 (2007) 111–22.
- [42] M. Romain, B. Thiroux, M. Tardy, B. Quesnel, X. Thuru, (2020). Measurement of Protein- Protein Interactions through Microscale Thermophoresis (MST), *Bio-protocol* 10 (2020) e3574.
- [43] K.M. Zak, P. Grudnik, K. Guzik, B.J. Zieba, B. Musielak, A. Dömling, G. Dubin, T.A. Holak Structural basis for small molecule targeting of the programmed death ligand 1 (PD-L1), *Oncotarget* 24 (2016) 30323–35.
- [44] K.M. Zak, P. Grudnik, K. Magiera, A. Dömling, G. Dubin, T.A. Holak. Structural biology of the immune checkpoint receptor PD-1 and its ligands PD-L1/PD-L2, *Structure* 25 (2017) 1163–1174.
- [45] L. Skalniak, K.M. Zak, K. Guzik, K. Magiera, B. Musielak, M. Pachota, B. Szelazek, J. Kocik, P. Grudnik, M. Tomala, S. Krzanik, K. Pyrc, A. Dömling, G. Dubin, T.A. Holak,

- Small-molecule inhibitors of PD-1/PD-L1 immune checkpoint alleviate the PD-L1-induced exhaustion of T-cells. *Oncotarget* 8 (2017) 72167–72181.
- [46] W.L. Jorgensen, J. Tirado-Rives. Molecular modeling of organic and biomolecular systems using BOSS and MCPRO, *J. Comput. Chem.* 26 (2005) 1689–1700.
- [47] G. Jones, P. Willett, R.C. Glen, A.R. Leach, R. Taylor. Development and validation of a genetic algorithm for flexible docking, *J. Mol. Biol.* 267 (1997) 727–48.
- [48] G. Vergoten, I. Mazur, P. Lagant, J.C. Michalski, J.P Zanutta. The SPASIBA force field as an essential tool for studying the structure and dynamics of saccharides, *Biochimie* 85 (2003) 65–73.
- [49] J. Chen, R. Chen, S. Huang, B. Zu, S. Zhang. Atezolizumab alleviates the immunosuppression induced by PD-L1-positive neutrophils and improves the survival of mice during sepsis, *Mol. Med. Rep.* 23 (2021) 144.

GRAPHICAL ABSTRACT



Pyrazolones

